NATIONAL AERONAUTICS AND SPACE ADMINISTRATION

Technical Report 32-1150

A 2000°F Lithium Erosion and Component Performance Experiment

L. G. Hays

D. O'Connor

Approved by:

D. R. Bartz, Manager
Research and Advanced
Concepts Section

JET PROPULSION LABORATORY

CALIFORNIA INSTITUTE OF TECHNOLOGY

PASADENA, CALIFORNIA

October 1, 1967

TECHNICAL REPORT 32-1150

Acknowledgment

Contents

Tables

Figures

Figures (contd)

Abstract

Results of a 2000°F lithium erosion experiment are presented, together with a discussion of performance of high temperature flow components and instrumentation. The main objective of the experiment was to evaluate the resistance to lithium impingement of candidate separator materials for a liquid metal magneto-hydrodynamic power system. After 100 hours duration with impingement velocities in the range of 110–150 ft/s, significant attack was observed on four hard materials which had exhibited long-term compatibility with static lithium. Another material (Cb-1%Zr alloy) was very resistant to impingement velocities of 150 ft/s and flow channel velocities up to 270 ft/s. Performance data for a helical induction pump and electromagnetic flowmeter operating at 2000°F were obtained which agreed well with predicted performance.

A 2000°F Lithium Erosion and Component Performance Experiment

I. Introduction

The long lifetimes required of electric-propulsion powerplants make cycles without rotating components or close tolerances attractive. Such a cycle under investigation at JPL is the liquid-metal magnetohydrodynamic system shown schematically in Fig. 1. In this cycle, cesium circulates in the vapor loop and causes a liquid metal, lithium, to circulate through an MHD generator in the liquid loop. The cesium leaves the radiator (or radiator-loop condenser) as condensate, flows through an EM pump and regenerative heat exchanger to the nozzle,
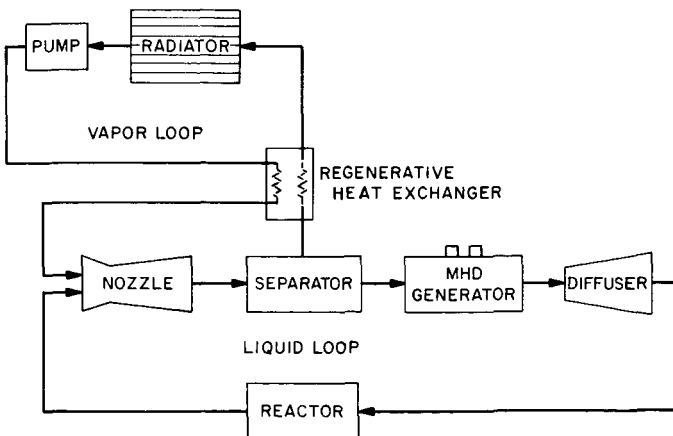
Fig. 1. Liquid MHD power conversion system

separates from the lithium in the separator, and returns to the radiator through the regenerative heat exchanger. The lithium leaves the separator at high velocity (typically 500 ft/s), decelerates through the production of electric power on the MHD generator, and leaves the generator with sufficient velocity (typically 300 ft/s) to return through a diffuser to the reactor (or reactor-loop heat exchanger) where the lithium is reheated.

The separator component utilizes the inertial forces of the impinging, high velocity, lithium droplets for separation from the cesium vapor and coalescence into a coherent stream. The successful operation of this component has been demonstrated with high velocity nitrogen-water mixtures (Ref. 1). However, some erosion of separator materials has been observed for these non-corrosive fluids at velocities lower than the final liquid metal system (Ref. 2). The combined corrosive and erosive environment of high velocity lithium at the temperature of interest ($\sim$2000°F) is a problem which must be resolved for long term system operation.

In this experiment impact velocities were below the range where major mechanical damage would be expected ($>$300–400 ft/s). Therefore, it was felt that accelerated chemical or dissolution effects would predominate. The rate of dissolution (or deposition) of a material by a liquid metal depends upon whether the process is limited

Specimen (number tested)	Compatibility[a] at 2000°F for indicated duration, hr					Comments
	100	500	1000	2000	3000	
Static tests						
BeO (2)		Poor				Partially dissolved; lithium penetration into ceramic
CaO (2)		Poor / Unusable	Poor / Unusable			Disintegration of 500-hr sample and significant mass transfer for 1000-hr sample; may be due to impurities
Sm_2O_3 (2)		Fair	Poor			Moderate mass transfer at 500 hr; dissolution and partial reduction at 1000 hr
ThO_2 (2)		Fair	Fair			Relatively unaffected; some dissolution at one corner; some cracking due to poor thermal stress resistance
Y_2O_3 (7)		Fair	Fair		Fair / Poor	Very minor dissolution at 500 to 1000 hr; significant mass transfer at 3000 hr from lower part of specimen; upper part of specimen unaffected
5% Y_2O_3, 95% ThO_2 (3)			Fair		Fair / Poor	Very minor dissolution at 500 to 1000 hr; significant mass transfer at 3000 hr from lower part of specimen; upper part of specimen unaffected
10% Y_2O_3, 90% ThO_2 (3)			Fair		Fair / Poor	Very minor dissolution at 500 to 1000 hr; significant mass transfer at 3000 hr from lower part of specimen
TiC (1)				Fair		Some cracking observed
ZrC (1)				Fair		Some cracking observed
$CaZrO_3$ (1)		Unusable				Very deep cracking and flaking
$BaZrO_3$ (1)		Unusable				Very deep cracking and flaking
AlN (3)			Poor		Poor	Heavy cracking
AlB_{12} (4)			Unusable			Completely disintegrated
BN (1)	Unusable					Completely disintegrated
MgO (1)	Unusable					Completely disintegrated
MgO · Al_2O_3 (1)	Unusable					Completely disintegrated
High-velocity (100- to 150-ft/sec) tests						
Cb–1% Zr (1)	Good					Slight wearing of tool marks; otherwise unaffected
W–2% ThO_2 (1)	Fair / Poor					Loss of ∼60 mils of material from tip
TiC (1)	Unusable					Severe cracking; loss of ∼30 mils of material from tip
ZrC (1)	Unusable					Severe cracking; loss of ∼¼ in. of material from tip
TaC (1)	Unusable					Severe chemical reaction; loss of ∼30 mils of material from tip

[a] Good: corners sharp and no measurable mass loss or cracking; useful for structural and nonstructural applications.

Fair: corners sharp, but a small amount of dissolution, mass transfer, and/or cracking present; useful for nonstructural applications; marginal for structural uses.

Poor: significant dissolution and/or cracking present; not useful for most applications.

Unusable: heavy dissolution, cracking, and/or chemical reaction.

Fig. 2. Compatibility of insulator and candidate separator materials with lithium at 2000°F

by the transfer of solute from the metal wall to the adjacent liquid layer or by the transfer through the liquid boundary layer to the external stream. The former case is commonly referred to as solution limited mass transfer while the latter is called diffusion limited mass transfer. For either case the material loss rate is a function of liquid metal velocity. For diffusion limited mass transfer the governing relations are analogous to empirical non-metal heat transfer relations. For example, for fully developed turbulent pipe flow the following equation holds:

$$Sh = 0.023\,Re^{0.8}\,Sc^{0.33} \qquad (1)$$

and the mass transfer coefficient (contained in the Sherwood number) is proportional to the flow velocity raised to the exponent, 0.8. For solution limited processes the dependency on velocity is not known, but the results of Ref. 3 appear to indicate a power of velocity which is higher than for diffusion limited transfer.

A large body of data on the compatibility of structural materials and ceramics with lithium has been generated. The results of more than 40 static capsule tests conducted at JPL at 2000°F on several ceramics and other hard materials for use for the separator or generator component are reported in Ref. 4. These results are summarized in Fig. 2. References 5 and 6 present other lithium compatibility results obtained by other investigators. These tests showed several refractory metal alloys, ceramics and carbides to be satisfactory for long-term use with 2000°F lithium. However, all of these data were taken under static or near static flow conditions.

Very few liquid metal tests have been conducted at high velocities because of lack of interest due to the higher attack rates. Several investigators have run tests to find the rate constants in both diffusion and solution limited processes (Ref. 3, 7, 8) but the maximum velocities have been limited to 25–30 ft/s.

One of the most promising structural materials for the liquid metal magnetohydrodynamic power system is columbium-1% zirconium alloy. This metal is readily available and has been used for complex high temperature liquid metal systems such as a lithium-boiling potassium turbine loop (Ref. 9). Results of testing a large Cb-1%Zr alloy flow loop with lithium at 2000°F for 10,000 h are reported in Ref. 10. No corrosion was experienced in flow components and piping where the velocities were 10–20 ft/s. Some surface roughening was reported in the heater where the velocity was 37 ft/s. However, grain boundary dissolution to a depth of 7 mils was

found in the tubes of a crossflow heat exchanger which were exposed to impingement of the flowing lithium. This result might be expected because of the high heat (and mass) transfer rates typical of the leading edge of a cylinder. It emphasizes the fact that a significant velocity and/or impingement effect is possible.

In order to assess the nature of the velocity effect for lithium at higher velocities (100–200 ft/s) a Cb-1%Zr alloy flow loop was constructed. This loop was designed to circulate lithium at 2000°F with a maximum velocity of 270 ft/s in two liquid nozzle throats. In addition, several test specimens of candidate separator materials were mounted at a location downstream of the nozzles where impingement velocities of about 150 ft/s were encountered.

A secondary purpose of the test was to obtain performance data on a helical induction pump and electromagnetic flowmeter and pressure and temperature instrumentation to be used in a more complex erosion loop in the future.

II. Experimental Apparatus

A. Test Section and Erosion Specimens

The test section geometry is illustrated in Fig. 3. Lithium flowing from the pump at high pressure entered the upstream section through a flow baffle. The flow was accelerated through two impinging flow nozzles to high velocities and formed a stream of droplets or a submerged jet which impinged upon five wedge-shaped test specimens.
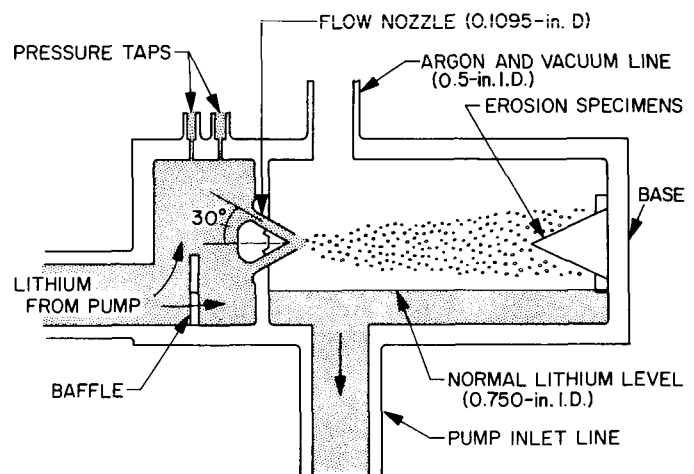

Fig. 3. Schematic of lithium erosion test section

The test materials were Cb-1%Zr, W-2%ThO$_2$, TaC, TiC, and ZrC. They were retained on a base by a tack-welded Cb-1%Zr holder. The carbides were fabricated from high purity powder by vacuum hot pressing at about 1700°C. Spectrochemical analyses of these carbides after pressing indicated a slight carbon deficiency from the stoichiometric amount. This is contrasted to the powder analysis which indicated about 5% free carbon. The carbon deficiency was probably caused by reaction of the carbon with residual oxygen and carbon monoxide during the hot pressing operation. The principal impurities present and their percentages were silicon, 70 ppm, nitrogen 40–70 ppm, and oxygen 380–720 ppm. The Cb-1%Zr and W-2%ThO$_2$ conformed to accepted purity standards for liquid metal usage: oxygen < 300 ppm, nitrogen < 200 ppm, carbon < 300 ppm, hydrogen < 15 ppm.

During the tests the liquid level in the specimen chamber was not accurately known. If the level were low a spray would be formed and the maximum impingement velocity would be 230 ft/s. If the level were high the jets would be submerged. For this case the maximum impingement velocity on the samples was estimated from Ref. 11 to be 150 ft/s. Calibration of the test section with water gave a flow coefficient of 0.930 for nozzle Reynolds numbers in the turbulent regime, but some-

what below those of the lithium test (2 × 10^5 vs 8 × 10^5). This value of flow coefficient was utilized with the pressure measurements to determine the lithium flow rate during the tests.

B. Test Loop

The primary flow loop and test section were fabricated of Cb-1%Zr alloy which requires a vacuum or inert gas atmosphere for operation at 2000°F. A schematic diagram of the flow circuit and auxiliary lines is shown in Fig. 4. Lithium was introduced to the test loop through two air actuated valves and a sintered stainless-steel filter. The lithium volumetric meter shown in Fig. 4 was used initially but proved to be unsatisfactory. A lithium-argon level was maintained in or above the test section and the rest of the loop was filled with lithium. Activation of the helical induction pump produced a flow of up to 11 gal/min of lithium through the flow meter section to the test section at a maximum pressure of 270 psia. Acceleration of the lithium to a maximum velocity of 270 ft/s in the two impinging flow nozzles was accomplished by maintaining the argon back pressure at about 25 psia. After impinging on the test specimens, the lithium was returned through the 1.0 in. OD pipe to the pump. Photographs of the loop before welding and after final installation are shown in Figs. 5 and 6.
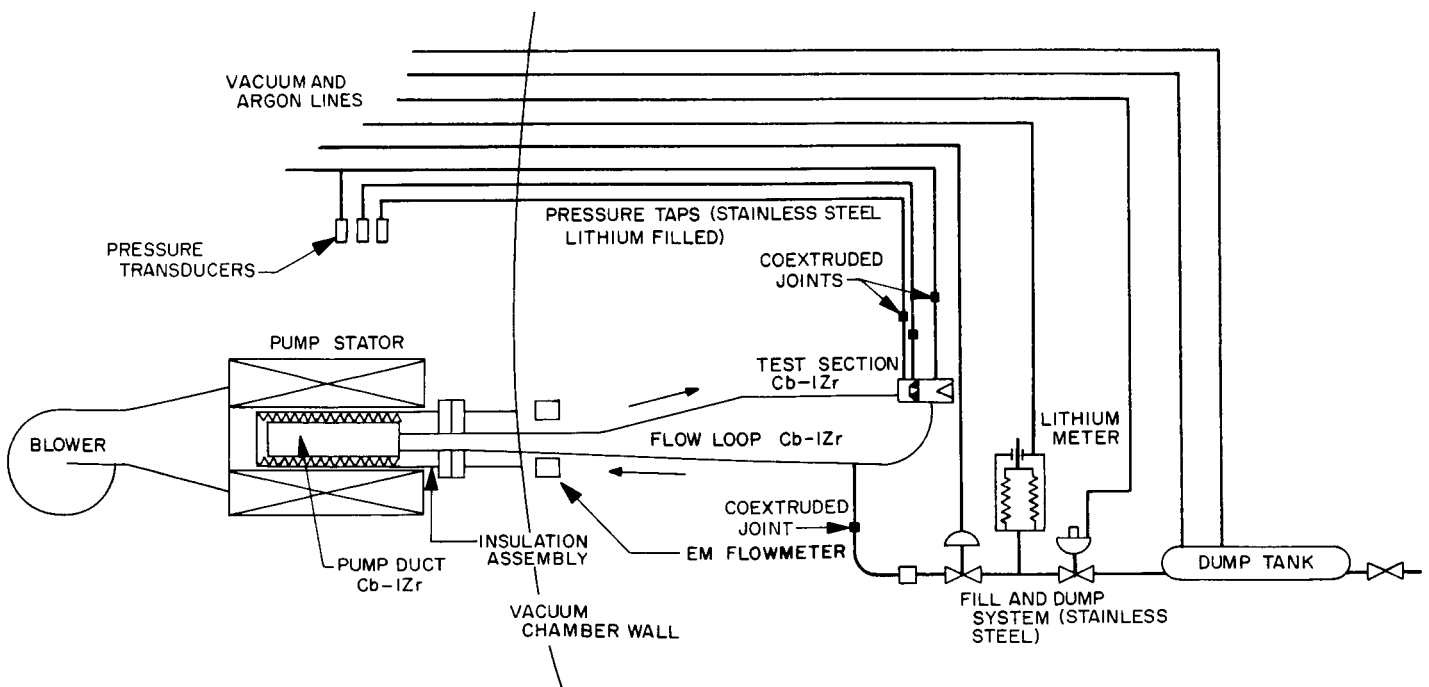
Fig. 4. Schematic of lithium erosion test loop
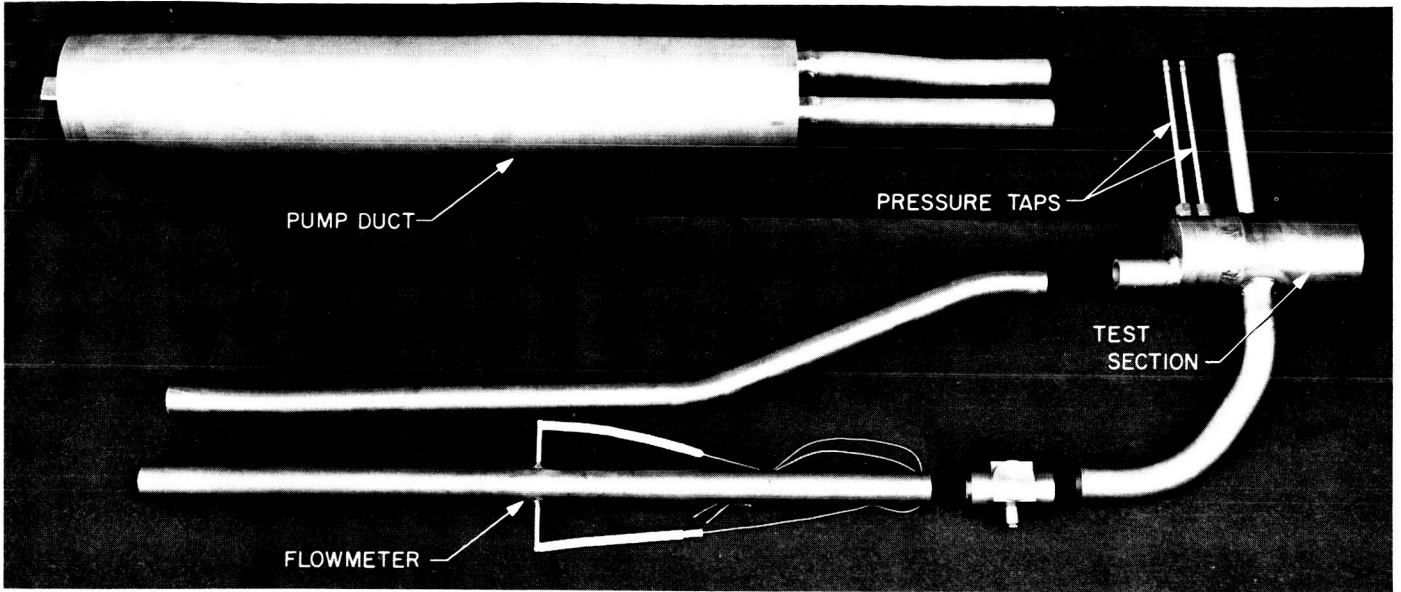
Fig. 5. Test loop before welding

PUMP DUCT

PRESSURE TAPS

TEST SECTION

FLOWMETER
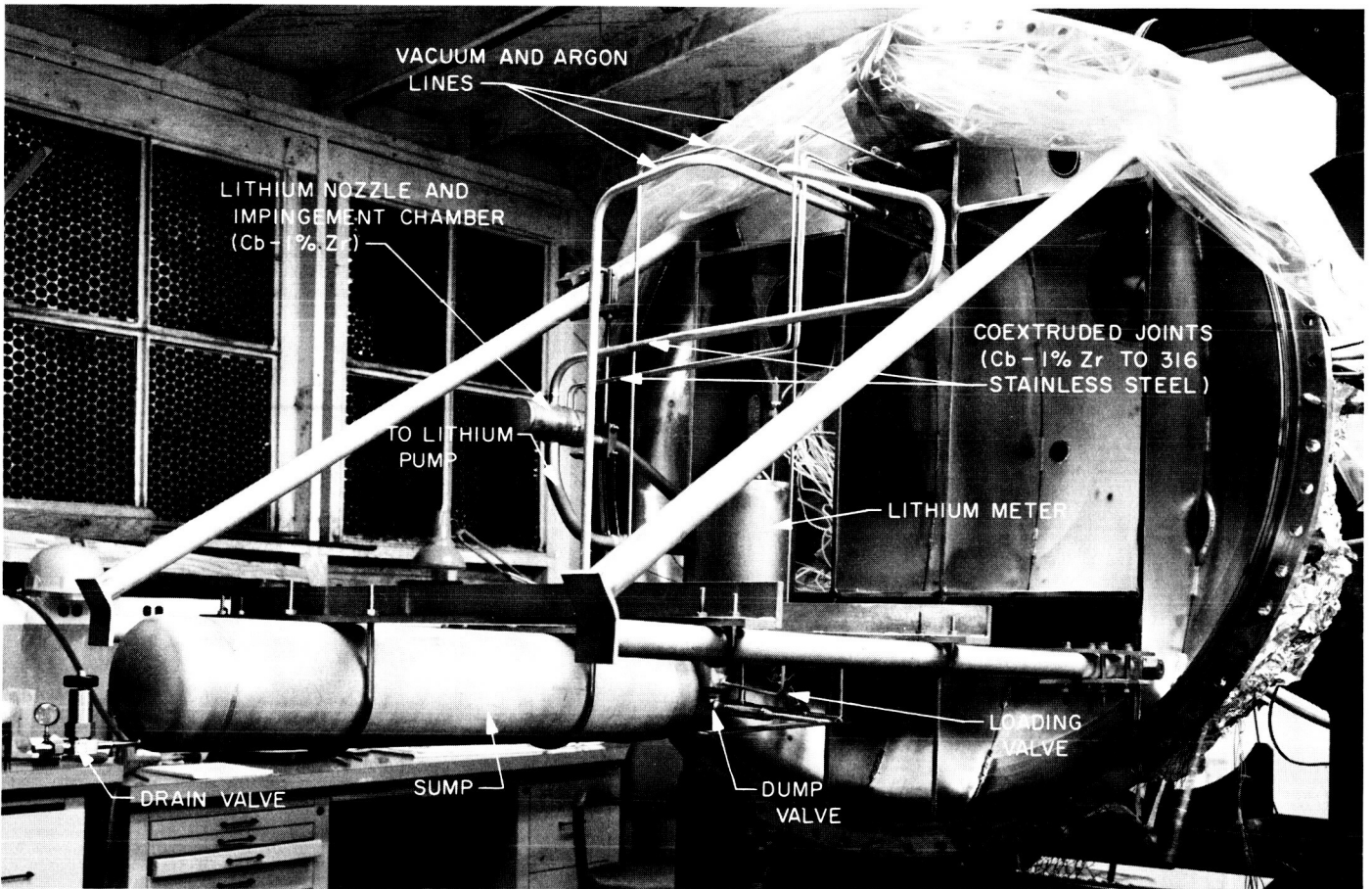
Fig. 6. Lithium erosion loop installed on door of vacuum chamber

VACUUM AND ARGON LINES

LITHIUM NOZZLE AND IMPINGEMENT CHAMBER (Cb – 1% Zr)

COEXTRUDED JOINTS (Cb – 1% Zr TO 316 STAINLESS STEEL)

TO LITHIUM PUMP

LITHIUM METER

DRAIN VALVE

SUMP

DUMP VALVE

LOADING VALVE

Evacuation and pressurization of the loop was accomplished through stainless steel vacuum and argon piping which was joined to the Cb-1%Zr through co-extruded Cb-1%Zr to 316 ss joints. Vapor traps installed to prevent lithium from freezing in these lines were successful under steady state conditions.

The most complex component of the flow loop was the helical induction electromagnetic pump supplied by General Electric Company. The design point for this pump at 2000°F is 270 psi pressure rise at a lithium flow rate of 16 gal/min. Basically the pump consisted of a Cb-1%Zr flow duct, an insulation assembly, and a three-phase stator. The insulation assembly in which the columbium alloy duct was contained served as an extension of the vacuum chamber. The stator was positioned on the outside of the insulation assembly and was air-cooled as shown in Fig. 7. For this test the pump also served as the heater. The test loop was designed so that the radiant heat loss at 2000°F would be equal to the induction heat input of the pump ($\sim$25 kW) at its design point. The radiant heat transferred from the loop was absorbed by cooling air circulating on the outside wall of the vacuum chamber.

The lithium used in the test loop was "reactor grade" quality, supplied with the manufacturer's analyses given in Table 1. No additional purification, other than filtration, was performed. All transfer operations were conducted in outgassed stainless steel lines through 5 micron filters under an argon cover gas containing less than 2 ppm oxygen. Table 1 furnishes the results of analyses of the lithium before and after the tests. The samples after the test should be of essentially identical composition. The low oxygen content after the tests is felt to be a good indication of low contamination prior to and during the test. The most significant fact about the remaining values is the large degree of scatter from one laboratory to another although the large values of tantalum and zirconium may be indicative of dissolution of these elements.

C. Vacuum Containment System

The vacuum chamber door formed the structural mounting for all test loop components. The chamber body, getter-ion pump and diffusion pump were installed on tracks for easy access to the test loop. The containment system, which is shown in Fig. 8, utilized all-metal

Table 1. Results of lithium analyses by weight percent

| Element | Pretest | Post-test | | | | | | | | | | |
	1	2	3	4	5	6	7	8	9	10	11
Li	99.97	—	—	—	—	—	—	—	—	99.	97.
Na	0.003	—	—	—	—	—	—	—	—	0.47	2.5
Fe	0.001	—	—	—	—	—	—	< 0.01	< 0.01	0.0034	0.0056
Ca	0.010	—	—	—	—	—	—	< 0.013	< 0.010	0.0093	0.013
Si	0.003	—	—	—	—	—	—	< 0.002	< 0.002	0.056	0.030
N	0.006	—	—	—	—	—	—	—	—	—	—
Cl	0.002	—	—	—	—	—	—	—	—	—	—
O	—	0.0062	0.0142	0.0123	—	—	—	—	—	—	—
Cb	—	—	—	—	0.034	0.098	< 0.002	< 2.3[a]	< 3.1[a]	—	—
Ta	—	—	—	—	2.27	2.7	< 0.005	—	—	—	—
Zr	—	—	—	—	0.37	0.24	< 0.005	—	—	—	—
K	—	—	—	—	—	—	—	—	—	—	< 0.010

1. Lithium Corporation of America.
2—4. General Atomics neutron activation analysis.
5. Cal-Colonial Chemsolve, spectrographic with lithium separation.
6. Cal-Colonial Chemsolve, spectrographic without lithium separation.
7. Materials Testing Laboratories, spectrographic.
8—11. Pacific Spectrochemical.
— Not measured.
[a]Sample contaminated by cutting columbium tube.
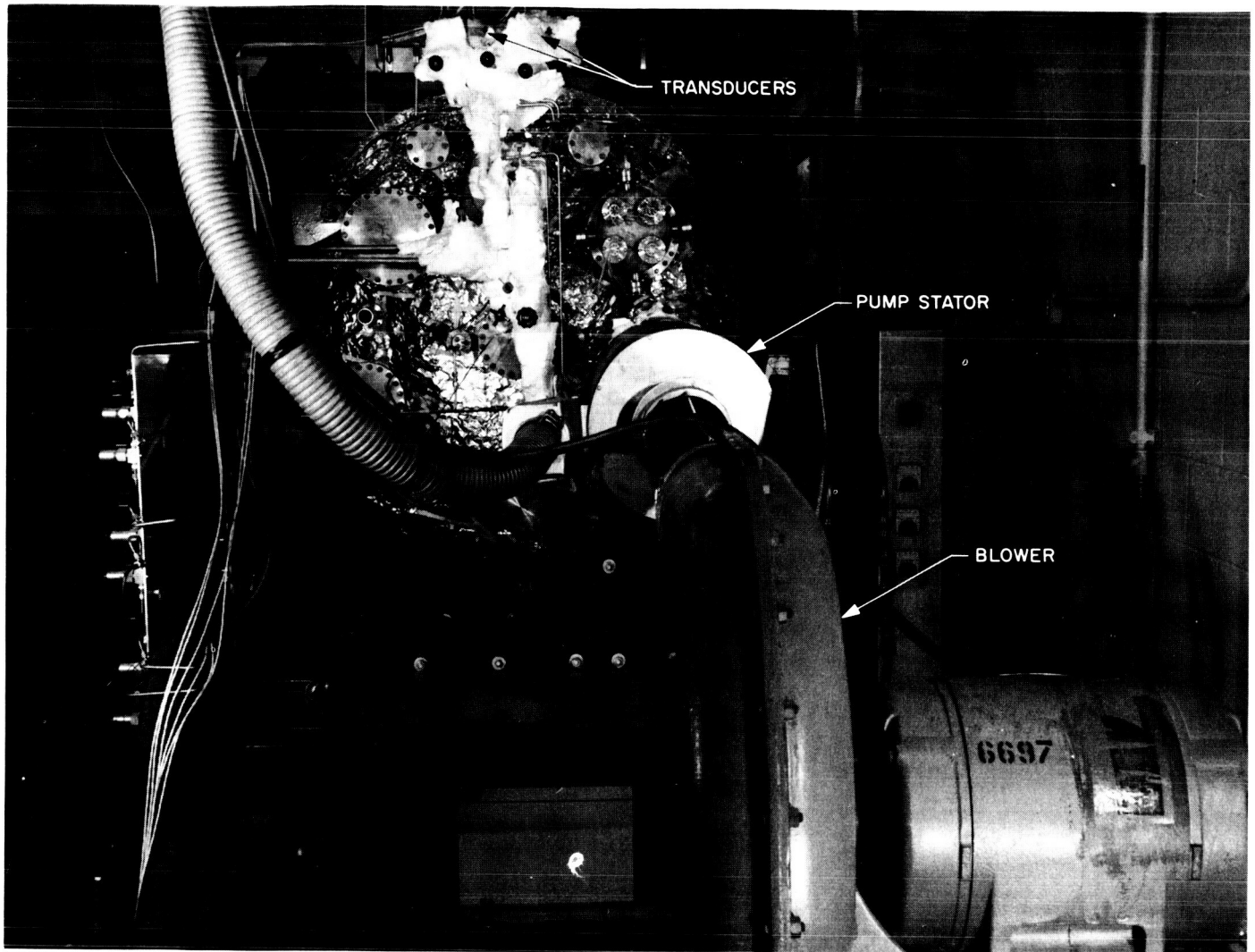
Fig. 7. Helical induction pump stator and blower

seals, except for the door O-ring which was Viton-A with water cooling. The vacuum chamber was traced with heaters and cooling lines. This enabled the chamber body to be maintained at 400–500°F during the test, eliminating the need for trace heaters on the loop to keep the lithium molten. The getter-ion pump, which was manufactured by General Electric Company, had a capacity of 1000 liter/sec. The Heraeus-Englehard diffusion pump, which was used for operation in the 10^{-3} to 10^{-4} torr range, had a capacity of 800 liter/sec.

D. Instruments and Controls

Temperature measurement on the loop was accomplished with tungsten 5% rhenium-tungsten 26% rhenium and chromel-alumel thermocouple pairs and with an optical pyrometer. The W5Re-W26Re thermocouples were bare wires which were spot welded under argon cover to the Cb-1%Zr wall and provided with radiation shielding.

The chromel-alumel thermocouples were swaged units having a tantalum sheath and were held in contact with the surface by spotwelded tantalum foil straps.

Since the primary loop was isothermal (to within 25°F), an optical pyrometer reading of the test section base was used to calibrate the thermocouples. A black body hole with a depth-to-diameter ratio of one was provided for this purpose. The only thermocouple which gave satisfactory agreement was the tantalum sheathed chromel-alumel unit.
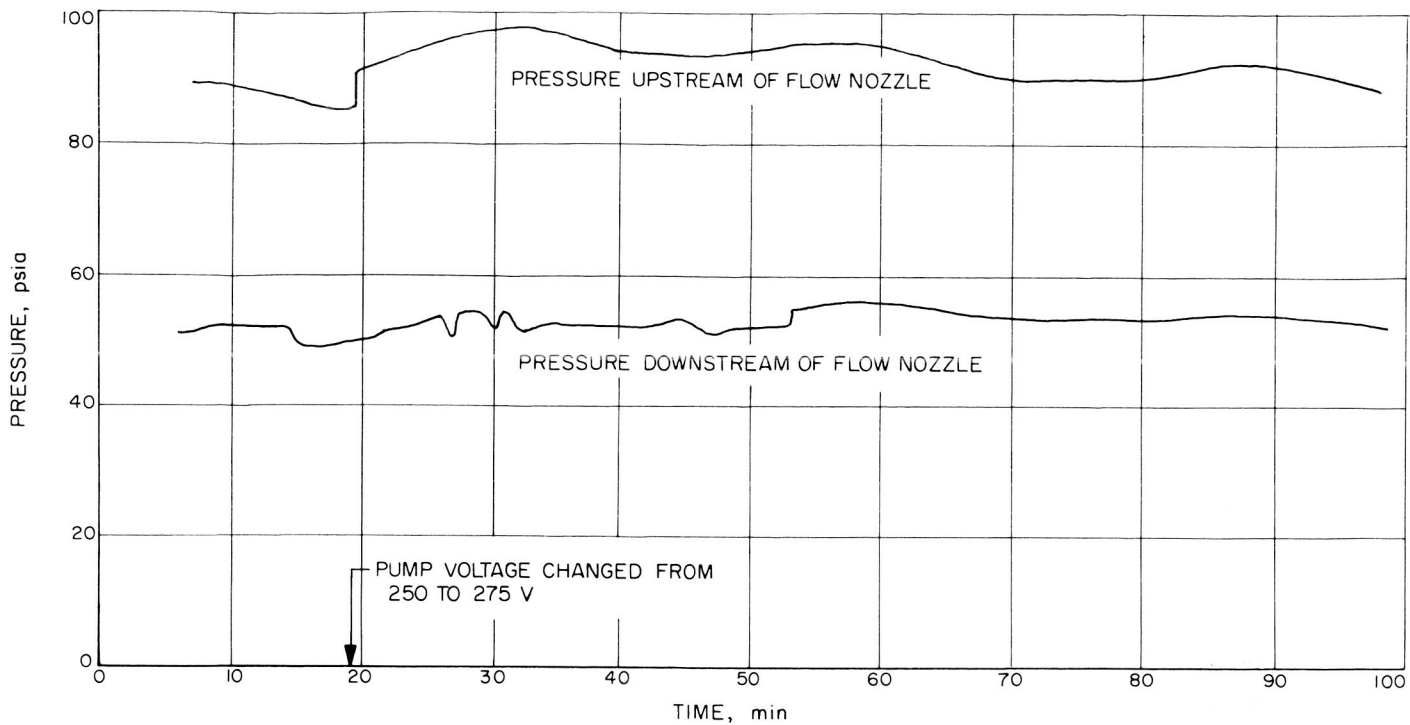
Fig. 9. Lithium loop pressures as a function of time

The chart contains the following labels:

- PRESSURE UPSTREAM OF FLOW NOZZLE
- PRESSURE DOWNSTREAM OF FLOW NOZZLE
- PUMP VOLTAGE CHANGED FROM 250 TO 275 V

Y-axis: PRESSURE, psia
X-axis: TIME, min
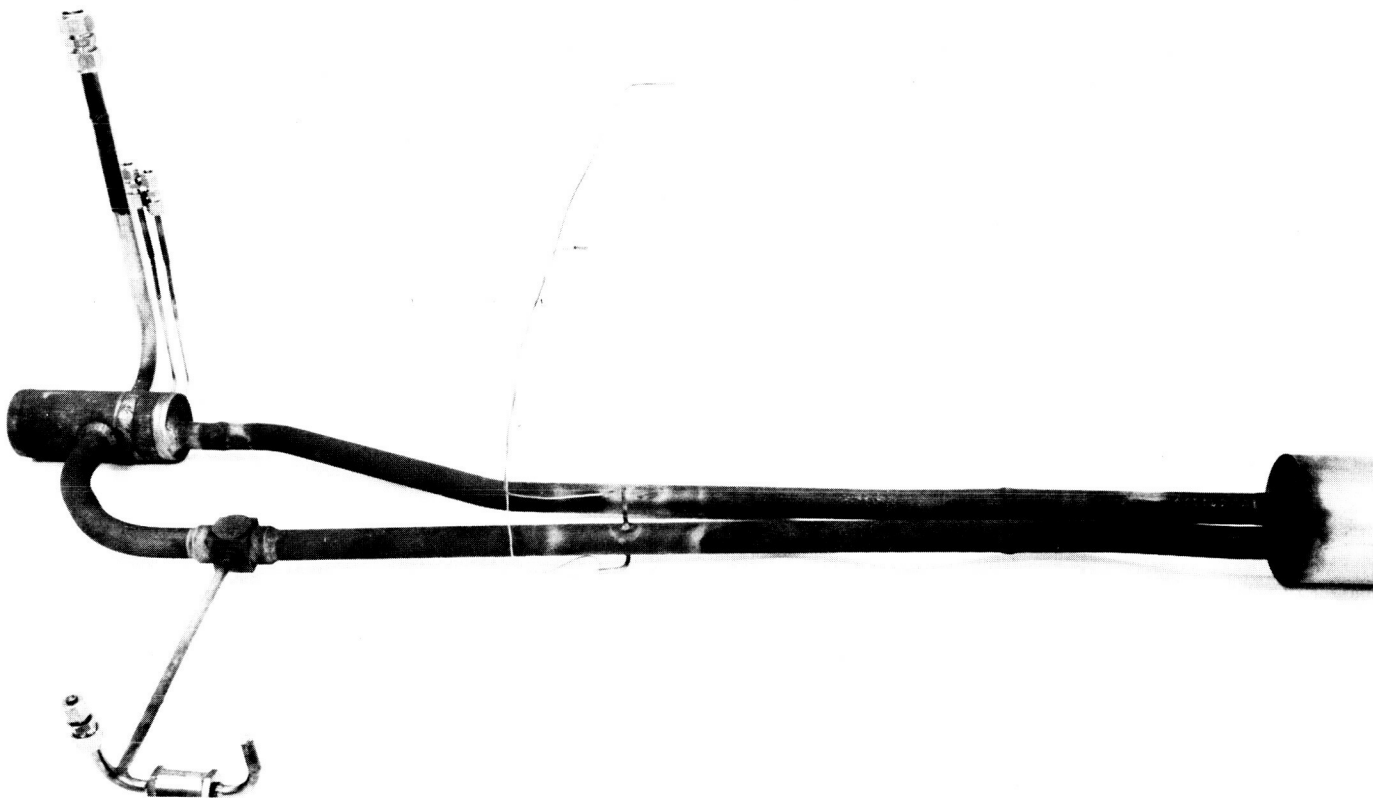
Fig. 10. Lithium test loop after oxidation at 1700°F

overheating of the copper gasket at this location. A rapid shutdown was made but the loop was severely oxidized. Figure 10 is a view of the test loop after this event.

The entire flow assembly was removed and grit blasted with aluminum oxide to remove the surface oxide layer, and then completely filled with lithium to insure proper pump operation.

The vacuum joint was modified to enable adequate cooling and internal insulation. After the lithium fill one of the pressure tap lines was inadvertently broken where it joined the test section body. A plug was welded over the hole using a rhenium gasket to seal the weld zone from lithium melted in the test section during welding.

The second attempt to operate was disrupted when one of the pressure transducers ruptured, resulting in a lithium leak. The lithium reacted with the quartz insulation, causing a fire. The cause of the failure was incomplete drainage of the lithium from the sensor cavity in the transducer. The subsequent remelting produced stresses which exceeded the strength of the transducer. To rectify this situation the transducers were replaced and the new units were filled with argon before the introduction of lithium. The resulting gas pocket produced complete expulsion of the lithium during subsequent drainage.

After replacement of the transducers and repair of the damaged auxiliary gas circuits the loop was again operated. This time steady flow and pressure readings were obtained and pump performance agreed well with predicted values. A lithium temperature of 2000°F was reached after 54 hours. The test was continued for 100 hours at 2000°F with a maximum flow rate of 11 gal/min, which produced a throat velocity of 270 ft/s. A photograph of the test section base at 1700°F is shown in Fig. 11. Shutdown was carried out after 100 hours at 2000°F because of lithium leaks from the repaired Cb-1%Zr pressure tap and from fittings used in the auxiliary, stainless steel lines. The leaks were small enough that the chamber pressure remained at 10^{-6} torr, but the volume of lithium lost and volume of argon introduced to maintain loop pressure was sufficient to result in some argon entrainment in the flow to the pump which once again caused a drop in performance. In addition the lithium caused short circuits in most of the thermocouples. Normal shutdown occurred over an eight-hour period. Data for this test period are tabulated in Table 2.

During the 54-hour period required to reach 2000°F an abrupt drop in flowmeter output occurred. Post test
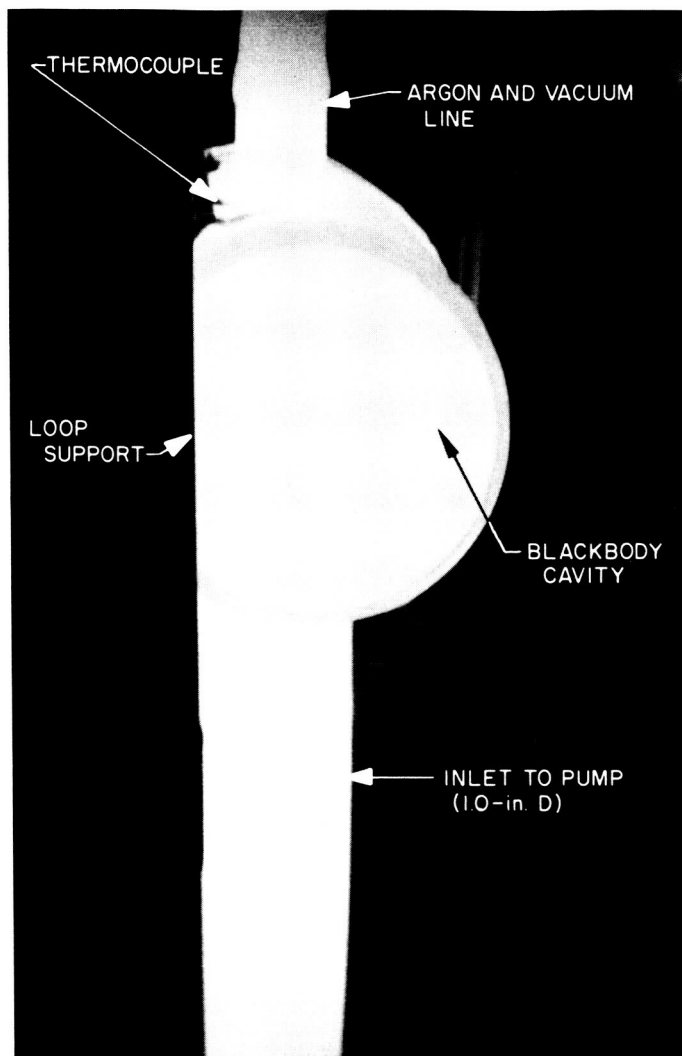

Fig. 11. Lithium test section at 1700°F

examination revealed the source of this disturbance to have been a piece of one of the test specimens which had broken off, circulated through the loop, and plugged one of the nozzles. Figure 12 is a radiograph of the test section taken after the test showing the piece of zirconium carbide plugging the nozzle.

B. Component Performance

Accurate readings by the pressure instrumentation were necessary for calibration of the pump and flowmeter. The use of cooled, lithium-filled pressure-tap lines provided the desired accuracy and reliability. None of the lines plugged during the test. This result is especially significant since the internal diameter was only 1/8 in. and since the temperature decreased from 2000°F to about 500°F within about three in. from the main

Table 2. Summary of lithium test data

Test point	Lithium[a] temperature, °F	Lithium[b] temperature, °F	Pump voltage, V	Pump power, kW	Upstream pressure, psia	Discharge pressure, psia	Nozzle pressure drop, psi	Lithium[c] flowrate, gal/min	Lithium[d] flowrate, gal/min	Lithium[i] velocity, ft/s
1	713	—[e]	66	1.07	34.7	23.6	11.1	3.12	3.20	55.0
2	792	—	79	1.51	39.0	23.8	15.2	3.79	3.75	63.3
3	867	—	90	1.90	43.2	23.6	19.6	4.16	4.27	72.1
4	957	—	100	2.28	48.7	23.5	25.2	—[e]	—[e]	82.3
5	970	—	110	2.68	51.0	23.6	27.4	5.06	5.08	85.7
6	1106	—	120	—[e]	56.7	24.0	32.7	5.61	5.58	94.4
7	1108	—	130	3.69	64.0	24.0	40.0	5.98	6.17	104.2
8	1126	—	140	4.20	64.0	24.0	40.0	6.35	6.17[f]	104.2
9	1180	—	150	4.82	64.0	24.0	40.0	5.25	6.19	104.7
10	1281	1330	170	7.08	98.0	24.0	74.0	6.08	8.48	143.2
11	1359	1395	193	7.26	107.0	24.2	82.8	6.46	9.01	155.2
12	—[e]	1472	210	8.50	121.8	26.0	95.8	7.11	9.72	164.2
13	1485	1516	220	9.25	139.0	26.0	113.0	7.63	10.59	178.8
14	1540	—[e]	226	9.84	143.5	26.0	117.5	7.82	10.80	182.5
15	1491	1515	226	9.89	142.0	25.0	117.0	7.85	10.78	181.9
16	1528	1550	235	10.61	151.0	24.0	127.0	8.11	11.24	189.8
17	1529	1599	—[e]	—[e]	152.0	24.0	128.0	8.20	11.30	190.7
18	1567	—[e]	247	11.62	158.5	25.1	133.4	8.60	11.61	196.0
19	1605	1649	260	12.62	171.5	21.9	149.6	8.88	12.24	207.0
20	—[e]	—[e]	263	12.78	180.8	23.8	157.0	—[e]	—[e]	—
21	1723	1642[h]	291	15.22	201.4	24.0	177.4	9.60	13.47	227.0
22	1788	1687	312	17.20	214.0	29.2	185.8	9.97	13.80	233.0
23	1880	—	338	19.8	236.0	26.5	209.5	10.48	14.70	248.0
24	1928	—	350	21.2	253.7	25.6	228.1	10.90	15.39	260.0
25[j]	1971	—	363	22.6	268.0	24.3	243.7	11.4 [i]	15.90	268.0
26	1796[g]	—	355	22.2	258.0	26.0	232.0	11.1	15.50	261.0
27	1536	—	350	21.5	253.5	26.0	227.5	11.0	15.50	260.0
28[k]	—	—	375	21.9	135.5	26.0	109.5	—	10.65	180.0

[a]W5Re vs W26Re thermocouple on surface.
[b]Pyrometer reading on black body hole.
[c]Electromagnetic flowmeter indication.
[d]Flow nozzle indication ($c_d = 0.930$).
[e]Reading not taken.
[f]Flow nozzle blockage occurred.
[g]Thermocouple degraded due to lithium short circuit.
[h]Window coated.
[i]Calculated from pressure difference.
[j]Start of 100 hr at 2000°F.
[k]Pump output dropped gradually from test point 27 to this value over the time period from 32 hr to 72 hr. It then remained nearly constant until shutdown at 100 hr. During this period the pump input power was constant.
[i]Flowmeter lead open. These values estimated from pressure readings and Fig. 14.
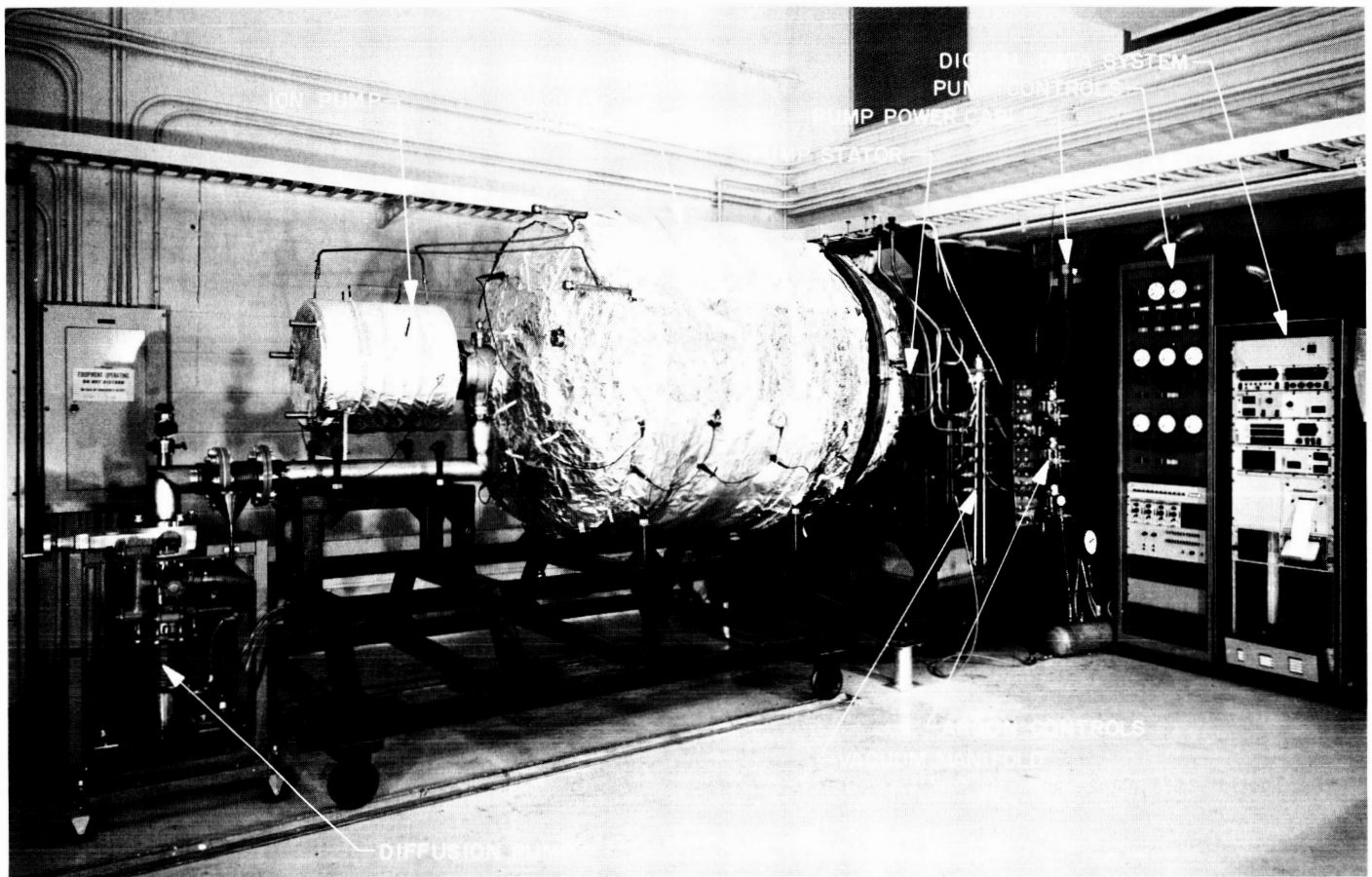
Fig. 8. Lithium erosion test facility

The flowmeter was a permanent magnet type constructed by MSA Research Corporation. The design output is 0.292 mV/gal/min at 2000°F. Twenty layers of dimpled Cb-1%Zr foil were applied to the flow tube to maintain the magnet at less than 800°F.

The lithium pressure was measured with Statham bonded strain gage transducers. The transducers were mounted outside the vacuum chamber and were maintained at 450°F by trace heaters. Lithium was brought directly from the loop through small diameter (⅛ in. ID) lines to the transducers. The lithium in the lines was maintained at 400–500°F by the vacuum chamber walls. The transducer installation is shown in Fig. 7.

Conventional vacuum gages, gas regulators and valves, and data display and recording equipment were used. The arrangement of loop controls and data display and recording equipment is shown in Fig. 8.

III. Operating Experience and Component Performance

A. Loop Operation

The test loop was operated for a total of 201 hours with lithium flow. Initial operation of the loop occupied 45 hours duration. After melting the lithium, which had previously been transferred to the flow loop, the temperature and flow rate were gradually increased to 1700°F and about 7 gal/min. This flow rate corresponds to a lithium jet velocity of 115 ft/s. However, it was apparent that the loop was not completely filled. Argon entrainment by the lithium returning to the pump was occurring. The pressure and flow readings oscillated by about 10% as shown in Fig. 9. Moreover, the pump was not providing a pressure rise consistent with the predicted value. The temperature was increased above the 1700°F value when a vacuum leak developed in the flange joining the pump insulation assembly to the vacuum chamber door. The cause of the leak was local
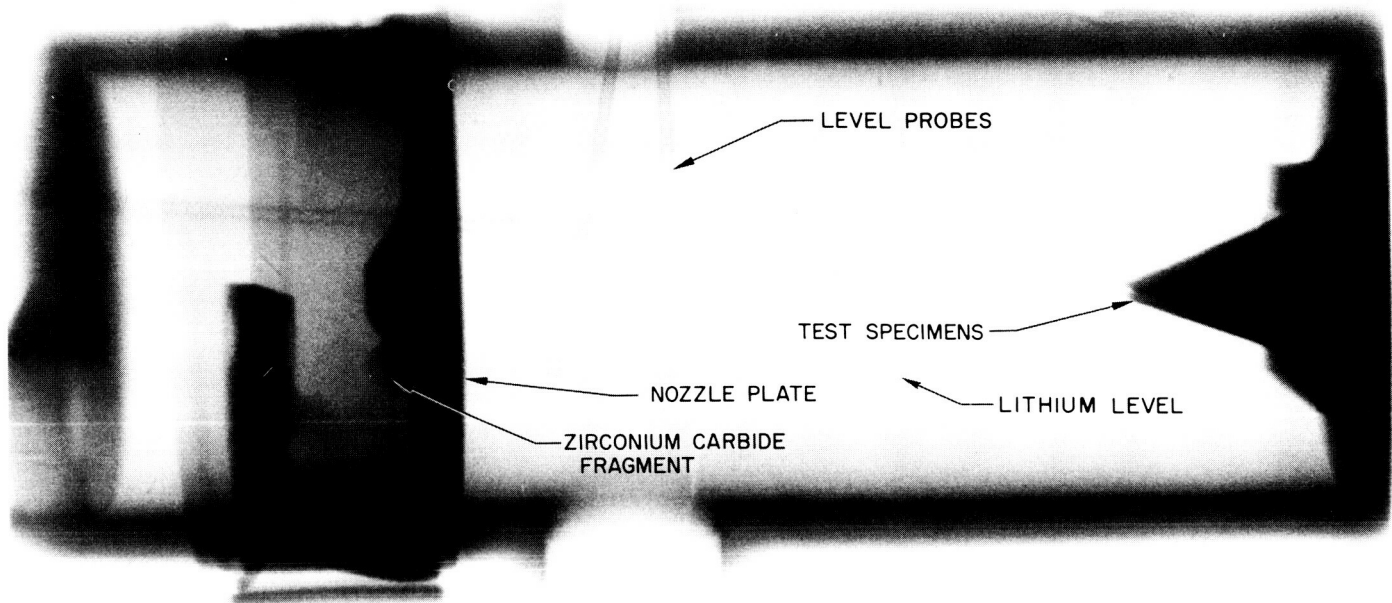
Fig. 12. Radiograph of test section showing plugged nozzle
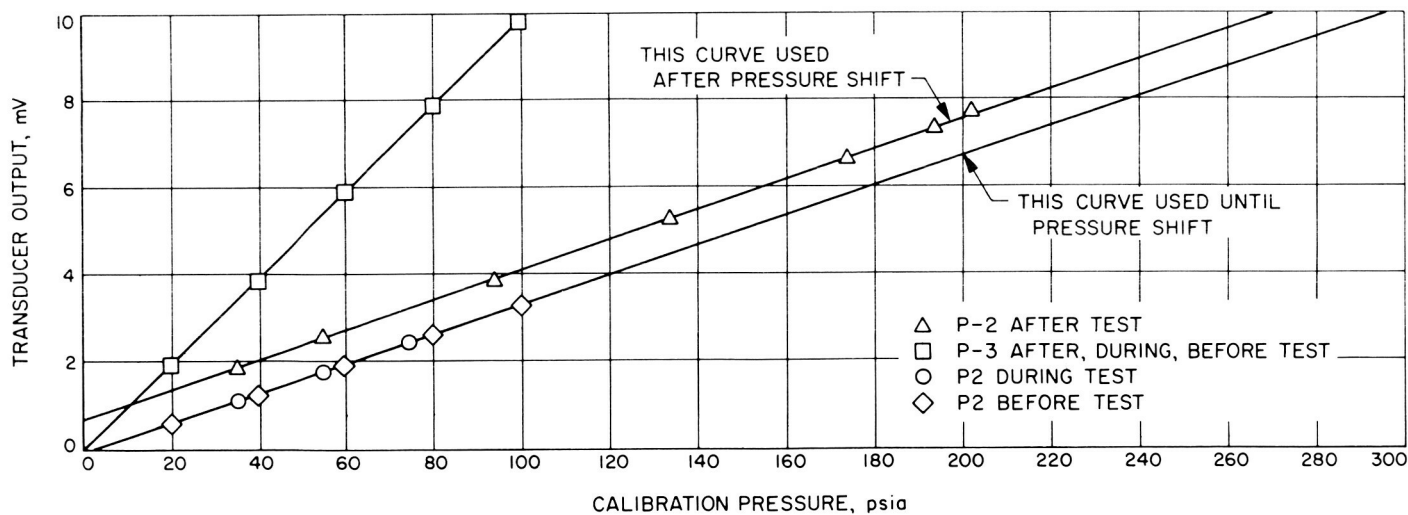

Fig. 13. Pressure transducer calibration curve

flow loop. The absence of plugging resulted from the high purity of the lithium.

The transducers were calibrated during the test with argon. The results were very repeatable except for a zero shift on one of the units, as shown in Fig. 13. The zero shift, which was about 8% of the full scale output, was abrupt and the transducer output remained linear after-

wards, so no loss of accuracy was encountered. The transducer outputs were linear and repeatable to within the reading uncertainty of about ½% of full scale for the calibrated Bourdon gauge used as the standard.

The flowmeter was calibrated using the transducer readings and the known discharge coefficient of the flow nozzles (0.930); Fig. 14 compares the flowrate indicated
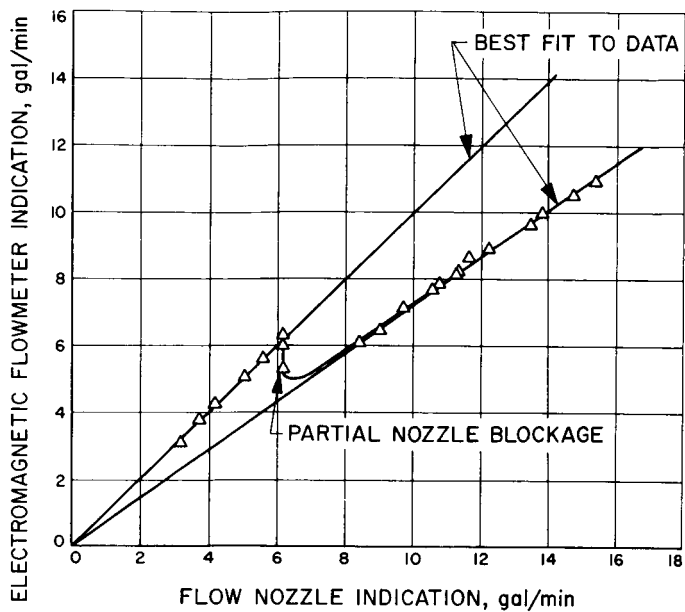
Fig. 14. Electromagnetic flowmeter calibration curve
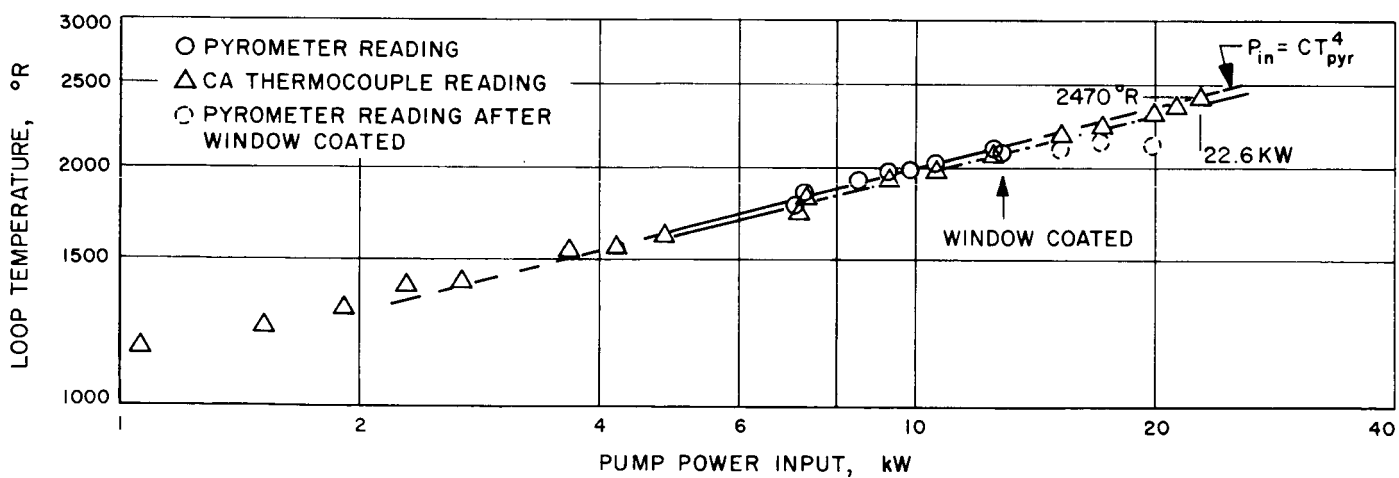
Fig. 15. Lithium temperature vs pump input power

by the electromagnetic flowmeter output using the curve supplied by the manufacturer with the flow indicated by the flow nozzle. Agreement to within 1% of the full scale readings was seen until the nozzle blockage described above occurred. The linearity of the curve before and after blockage and the zero origin of both curves lend confidence to use of the flowmeter reading instead of the flow nozzle indication after blockage.

Thermocouple performance during the test was less satisfactory. Eventual failure or erratic readings for several key thermocouples occurred during the test. The most prevalent cause of failure was inadequate means of attachment.

Comparison of the thermocouple reading with the optical pyrometer reading gave an agreement of within 20°F to 70°F in the range of 1500–1650°F. However, the pyrometer reading was only accurate until the window coated at about 1700°F. Extrapolation of the curve of pyrometer reading (which was taken as the true temperature) versus thermocouple reading to the thermocouple reading of 1971°F gave an estimated true temperature of 2010°F for the 100-hour run. During the later part of the 100-hour run the thermocouple was short-circuited by lithium which had leaked from the loop. The power input to the pump was held constant for the run and was used to estimate the temperature from the previous temperature readings.

The dependence of lithium temperature on the power input to the induction pump is shown in Fig. 15. As expected, the temperature is proportional to the ¼ power of the input power at higher temperatures. The maximum temperature of 2010°F was attained with a power input of 22.6 kW.

The helical induction pump provided completely satisfactory performance for the duration of this test. The output was smooth and controllable and conformed closely to the manufacturer's predictions. In Fig. 16 the relationship between measured pressure rise and lithium flow is superimposed on the calculated pump characteristic curves of pressure rise vs flowrate. The test points for 66 V, 140 V, 220 V and 321 V fall close to the theoretical curves for 68 V, 142 V, 223V, and 315 V, respectively. Since the nozzles had a fixed area and no valves were used it was not possible to vary the flow rate at constant voltage for a full comparison with the curves. The maximum pressure rise was 244 psi with an input voltage of 363 V. The applied voltage and pressure rise limit was
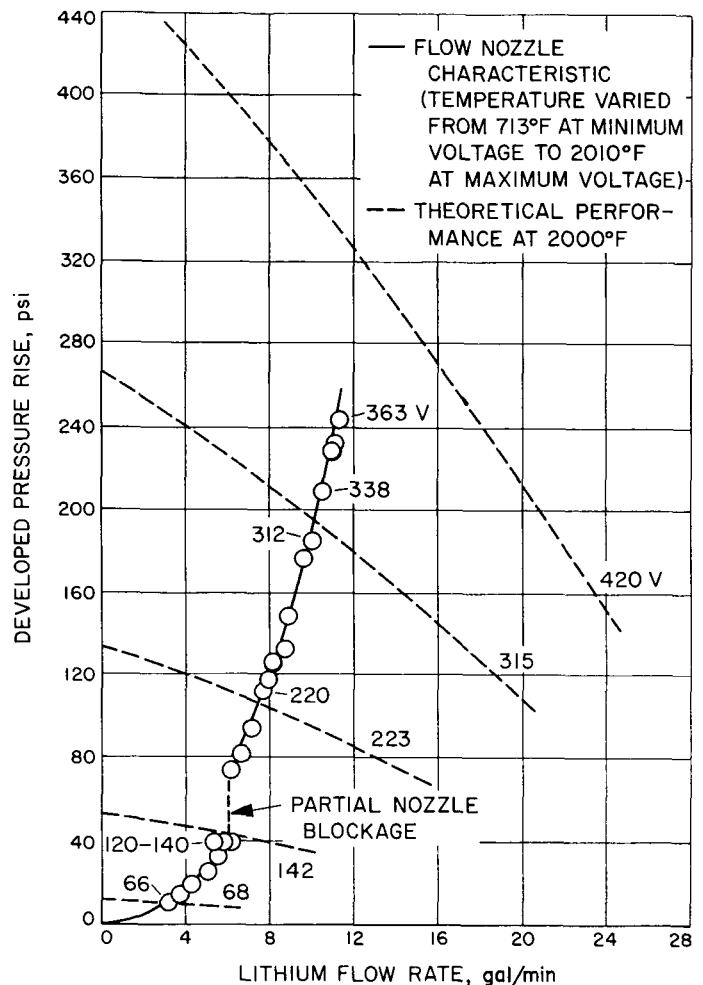

Fig. 16. Performance of lithium pump

established by the heat transfer area from the loop and the chosen temperature limit of 2000°F.

IV. Erosion Results

A. Impingement

The effects of high velocity lithium impingement on the test materials may be seen in Fig. 17. The only material which was relatively unaffected by 100 hours of exposure was Cb-1%Zr, which is number two in the figure. The thoriated tungsten specimen, number three, lost about 60 mils of material from the tip and was discolored. Specimen number five, (zirconium carbide), lost the entire top portion of the wedge. In addition the surface was discolored and heavily cracked. The tantalum carbide, number 4, lost about 30 mils from the tip and was discolored and cracked. The smooth appearance of
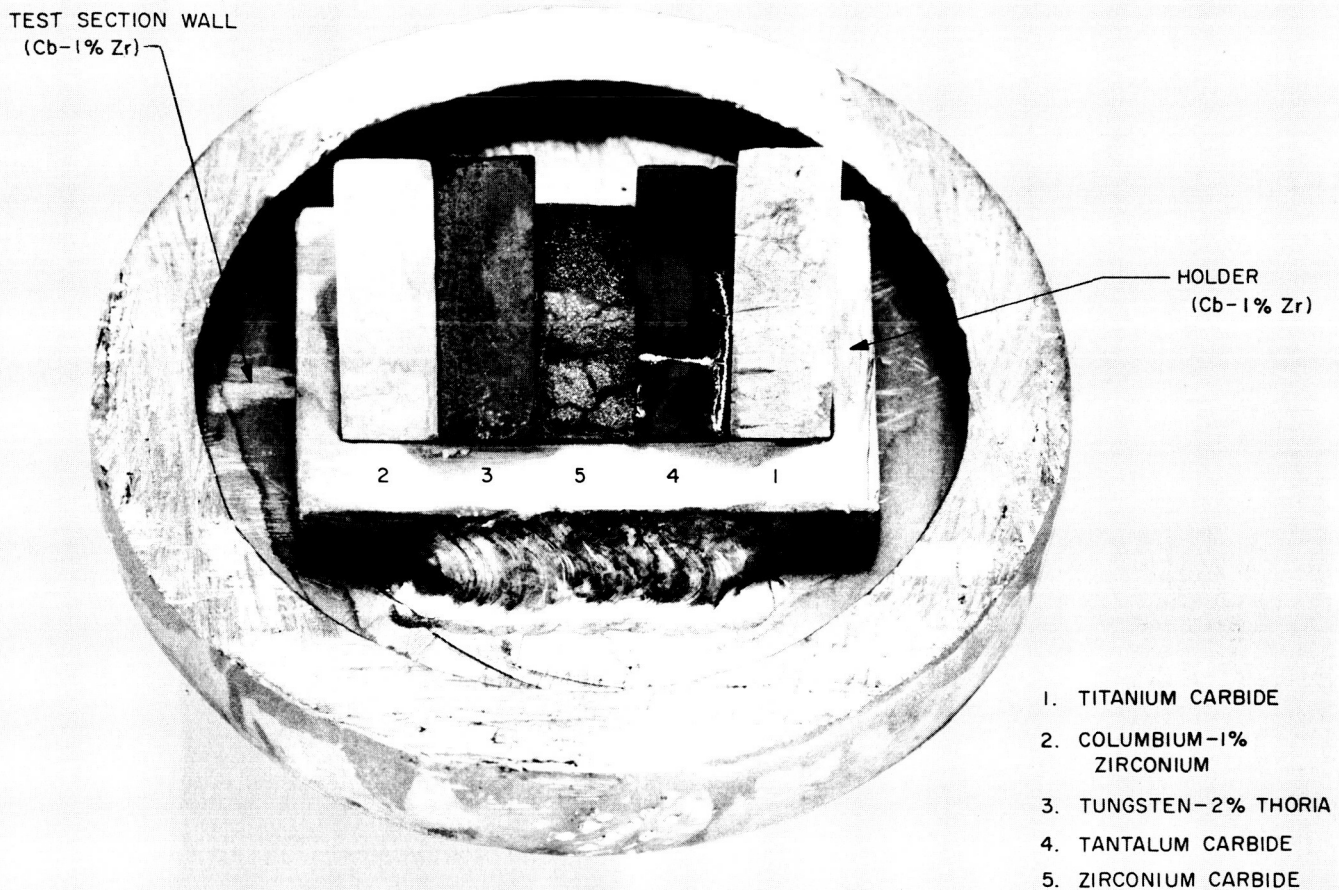
Fig. 17. Erosion test specimens after exposure to high-velocity lithium for 100 hr at 2000°F

the tip and post-test analyses show that the lithium reacted with the tantalum carbide. The remaining material, titanium carbide number 1, lost only a few mils from the tip but was heavily cracked and underwent damage on the inclined surface. The slightly greater mass flux of liquid to the center wedges may be a factor in their heavier damage. However, the impingement on the Cb-1%Zr specimen should have been identical to that on the titanium carbide, which was heavily damaged.

Figures 18–22 provide magnified views of the tips of all the materials before and after exposure to lithium and Figs. 23–27 show the inclined face after exposure. The exception is zirconium carbide which only has the before view of the tip since massive failure occurred.

Comparison of the before and after pictures for columbium-1% zirconium (Figs. 18 and 23) shows the

width of the tip to be the same. A small chip is missing which may have been due to an existing defect in the material. The grinding marks, although somewhat dulled, still are evident over the entire inclined surface.

The remaining structure of the W-2%ThO$_2$ specimen Figs. 19 and 24 has a jagged appearance, suggesting that the attack was predominately mechanical in nature. An electron micro-probe analysis of this specimen and the zirconium carbide specimen indicated the presence of tantalum on the discolored surfaces. The grinding marks exist to the broken surface.

Figures 20 and 25 show the zirconium carbide to be very heavily cracked after the test. The nature of the cracks and the presence of zirconium in one of the post-test analyses of lithium (Table 1) suggests an accelerated chemical attack to have occurred.

0.010 in.
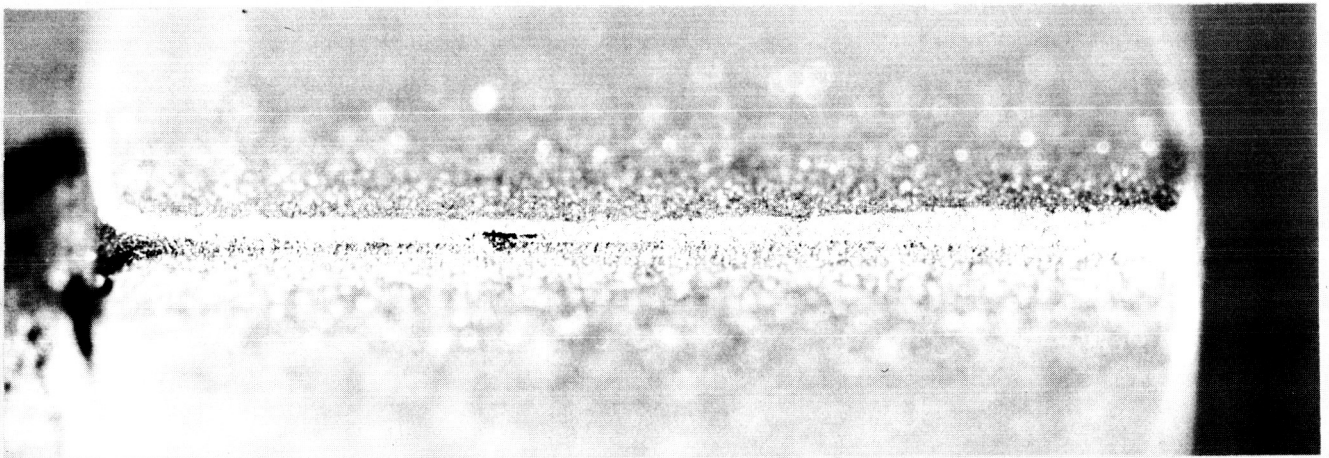
BEFORE EXPOSURE

AFTER EXPOSURE

Fig. 18. Columbium-1% zirconium wedge tip before and after exposure to high-velocity lithium for 100 hr at 2000°F
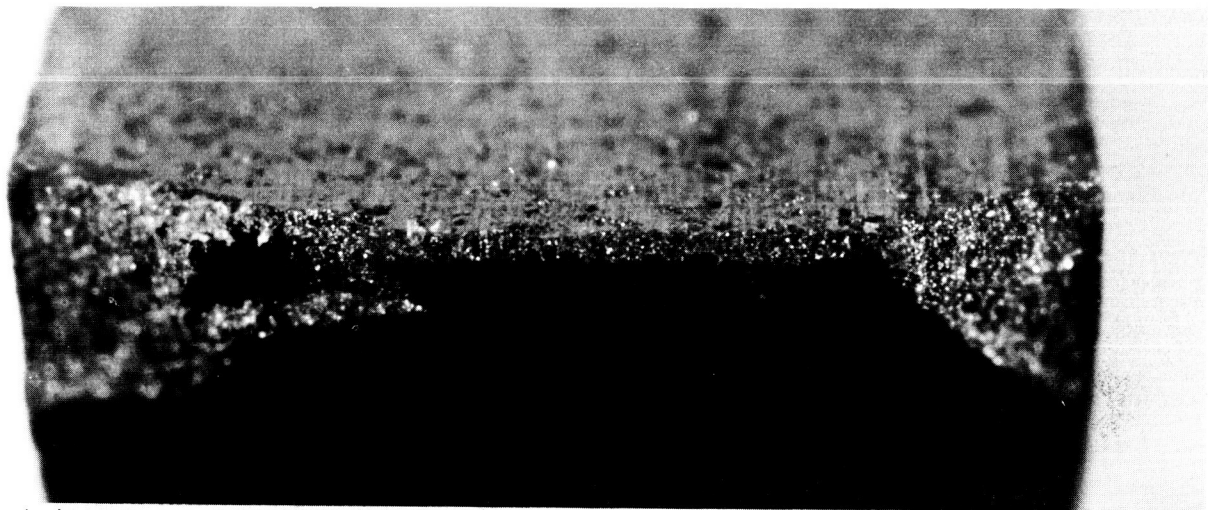
0.010 in.

BEFORE EXPOSURE

AFTER EXPOSURE

Fig. 19. Tungsten-2% thoria wedge tip before and after exposure to high-velocity lithium for 100 hr at 2000°F
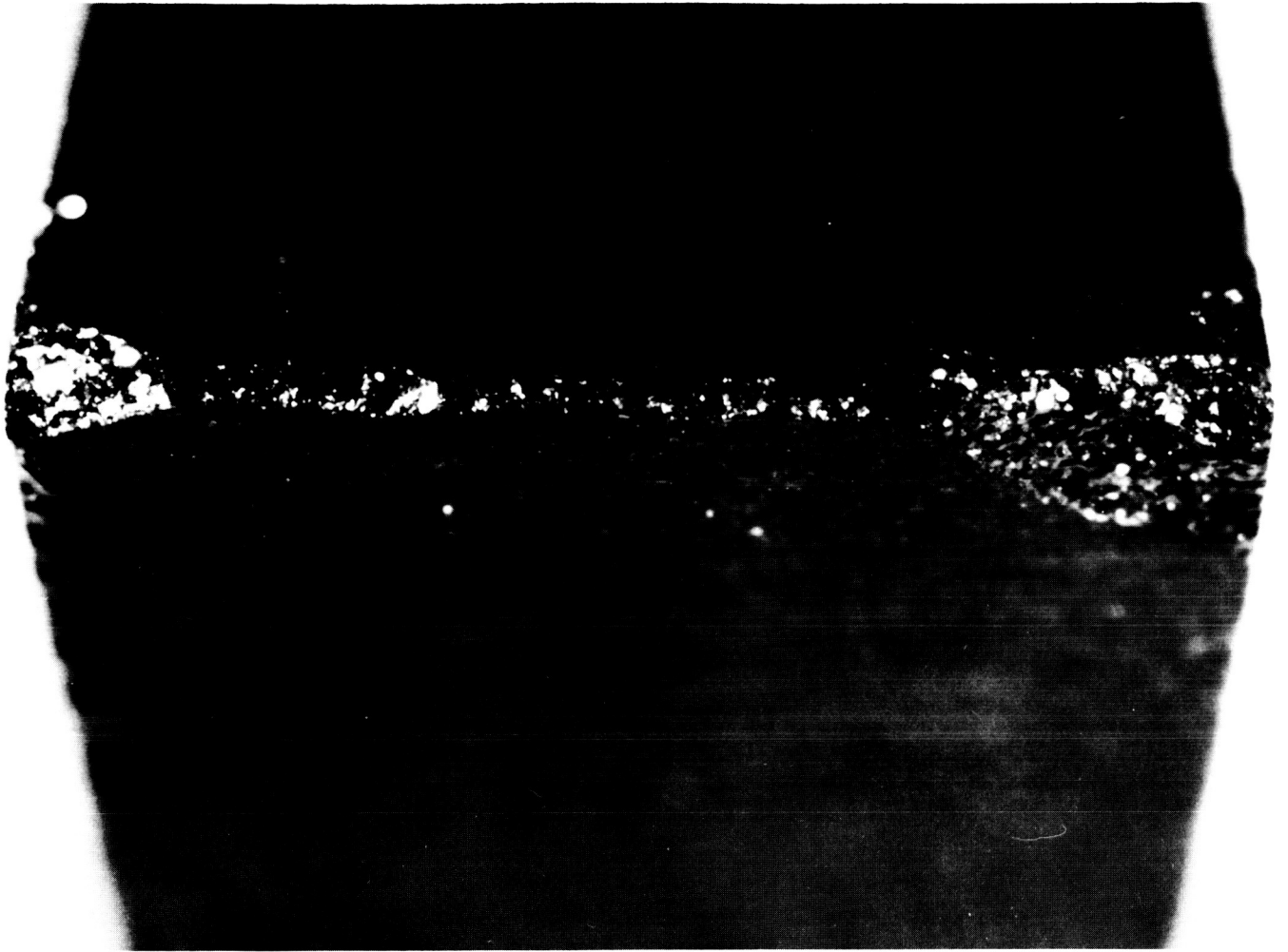
Fig. 20. Zirconium carbide wedge tip before exposure to high-velocity lithium for 100 hr at 2000°F
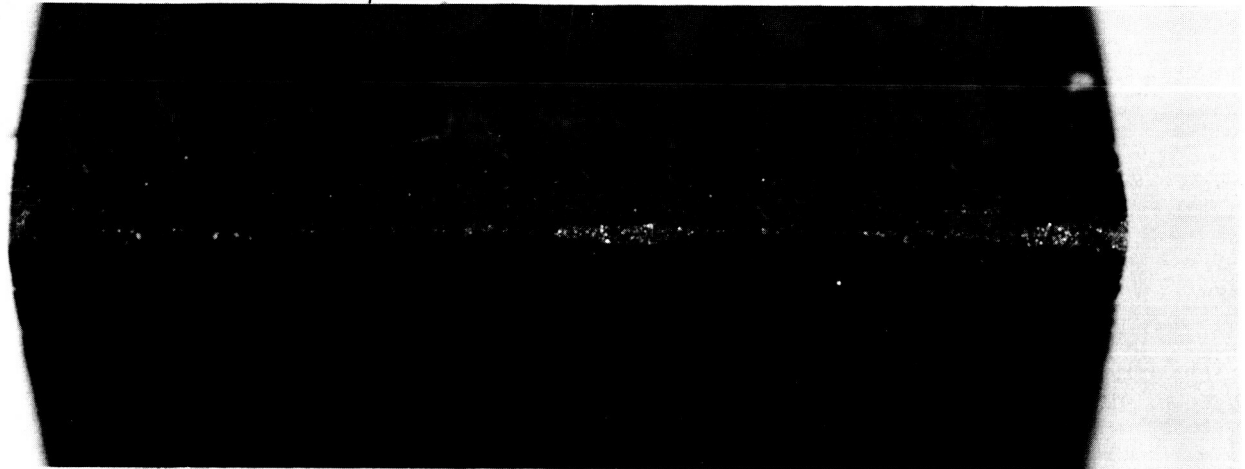
BEFORE EXPOSURE
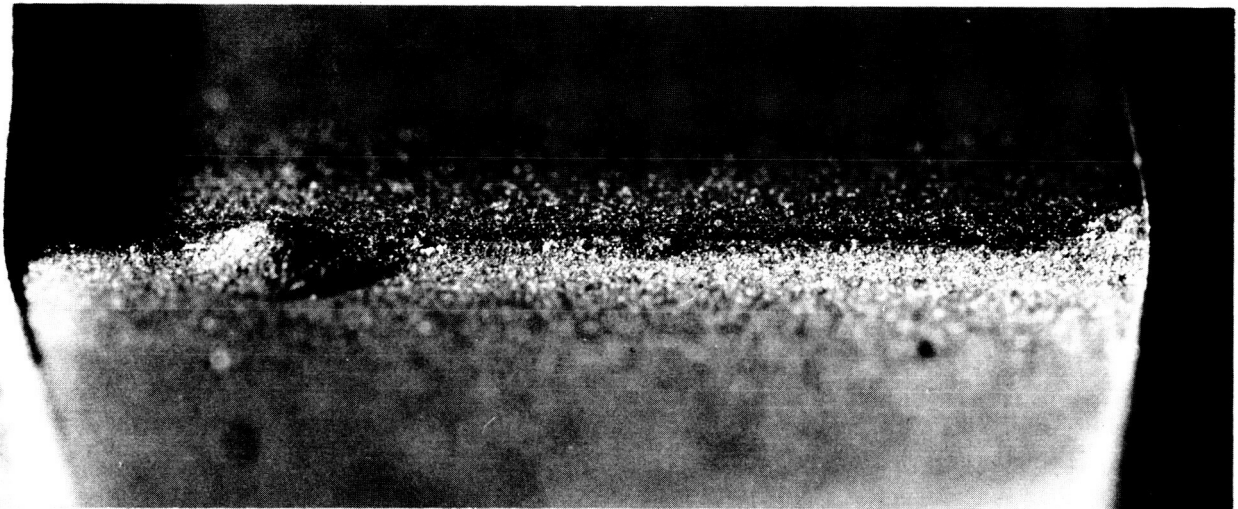
0.010 in.

AFTER EXPOSURE

Fig. 21. Tantalum carbide wedge tip before and after exposure to high-velocity lithium for 100 hr at 2000°F
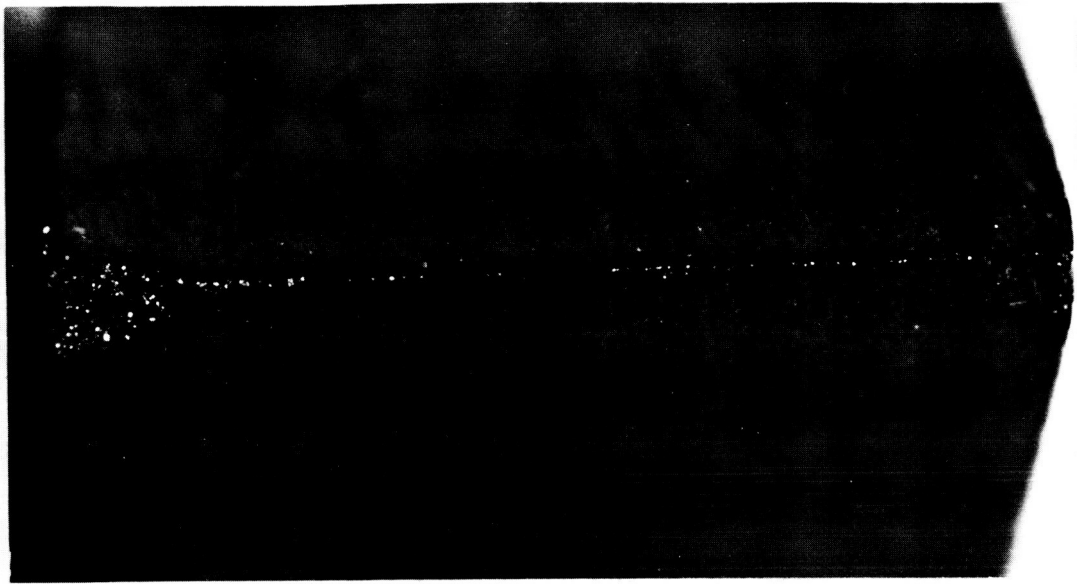
BEFORE EXPOSURE

0.010 in.

AFTER EXPOSURE

Fig. 22. Titanium carbide wedge tip before and after exposure to high-velocity lithium for 100 hr at 2000°F
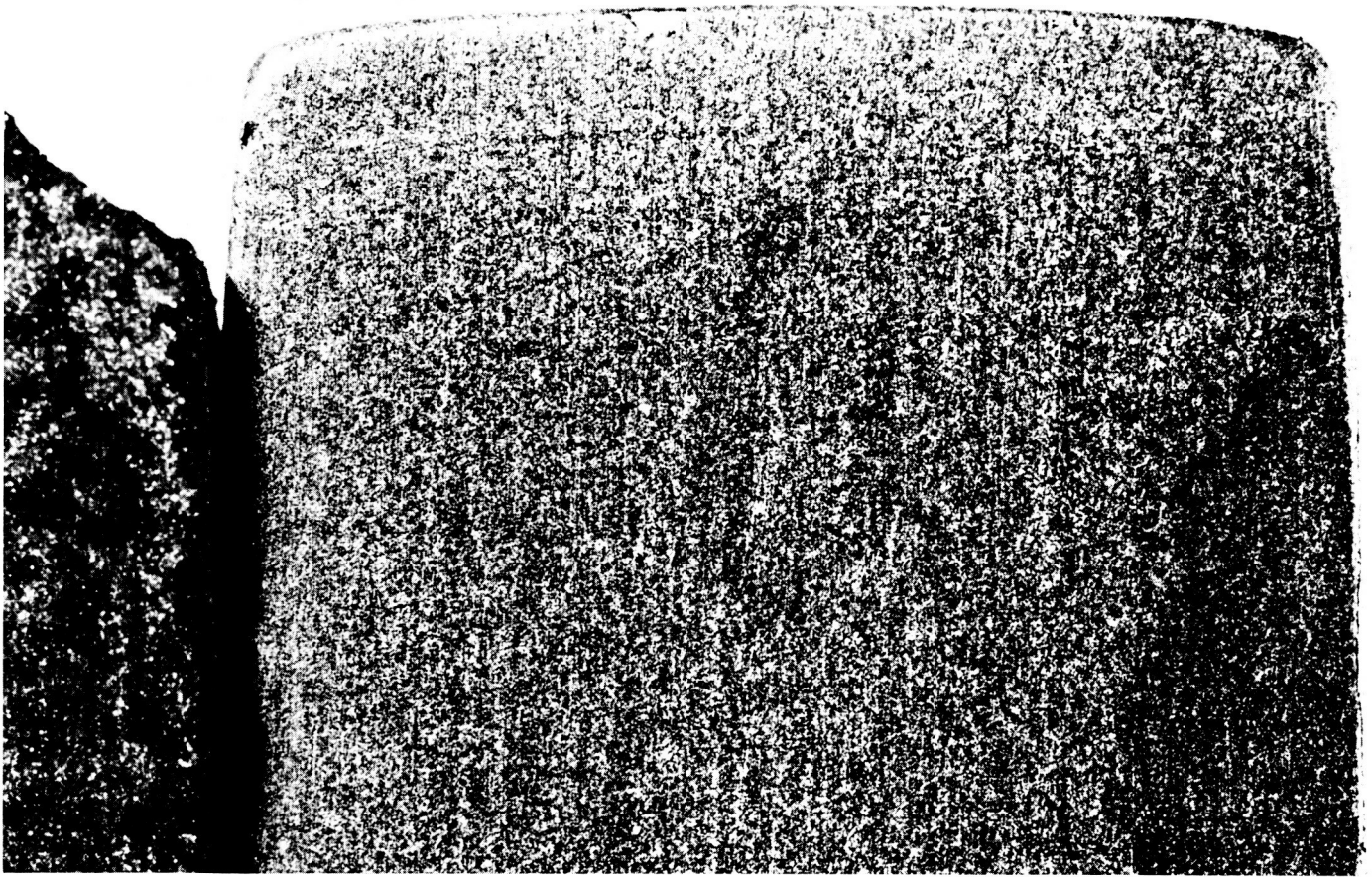
Fig. 23. Columbium-1% zirconium wedge face after exposure to high-velocity lithium for 100 hr at 2000°F
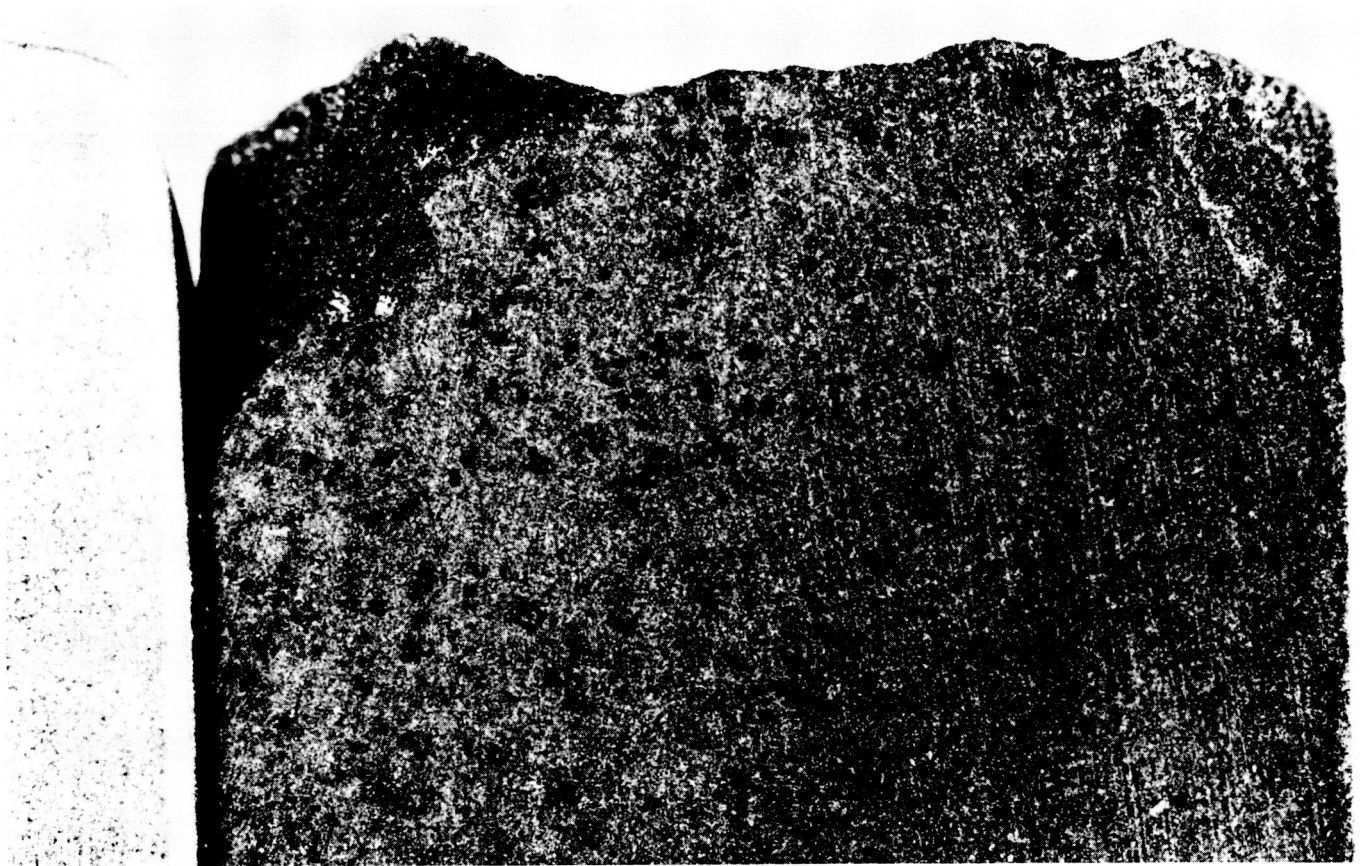
Fig. 24. Tungsten-2% thoria wedge face after exposure to high-velocity lithium for 100 hr at 2000°F
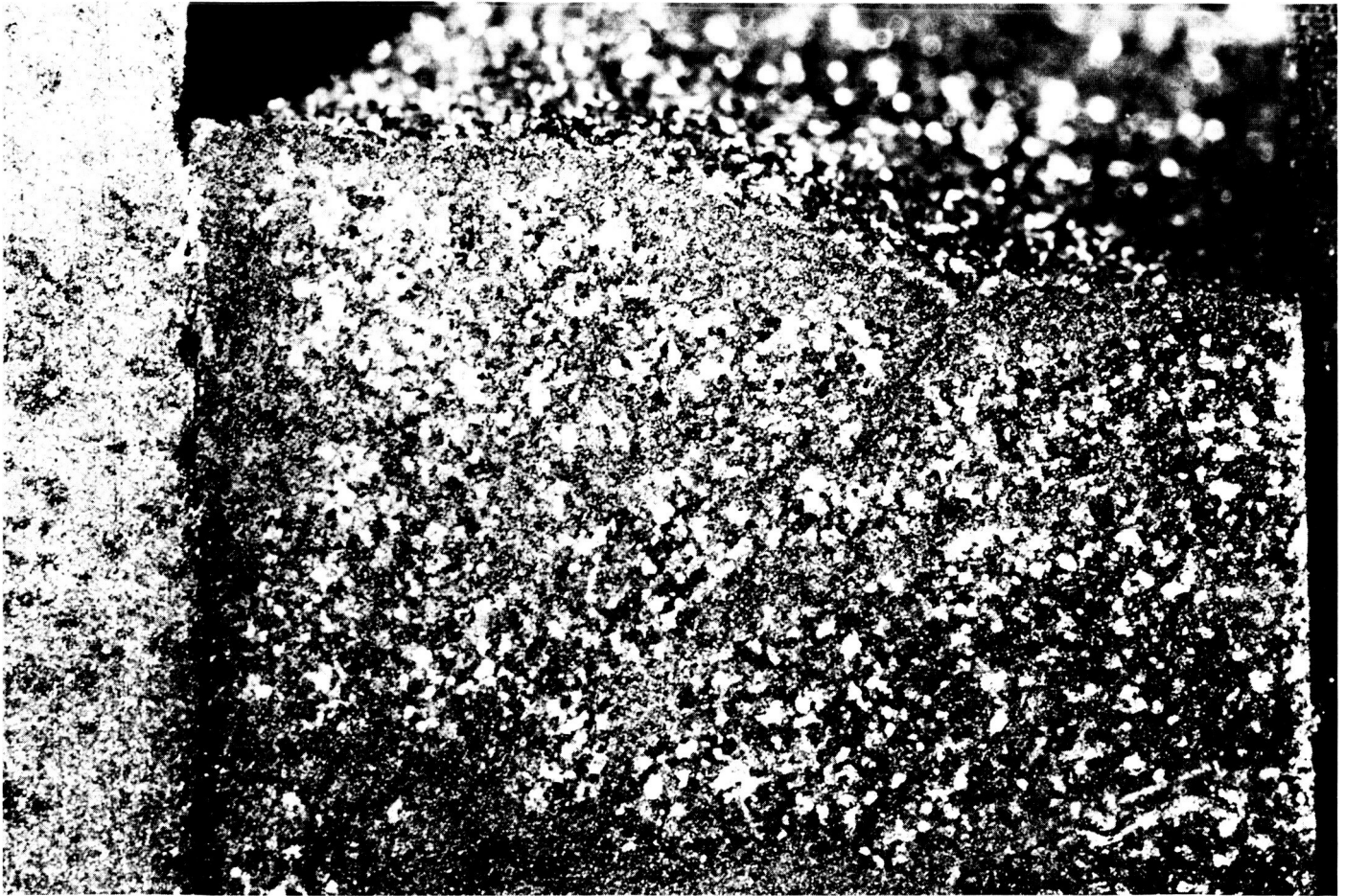
Fig. 25. Zirconium carbide wedge face after exposure to high-velocity lithium for 100 hr at 2000°F
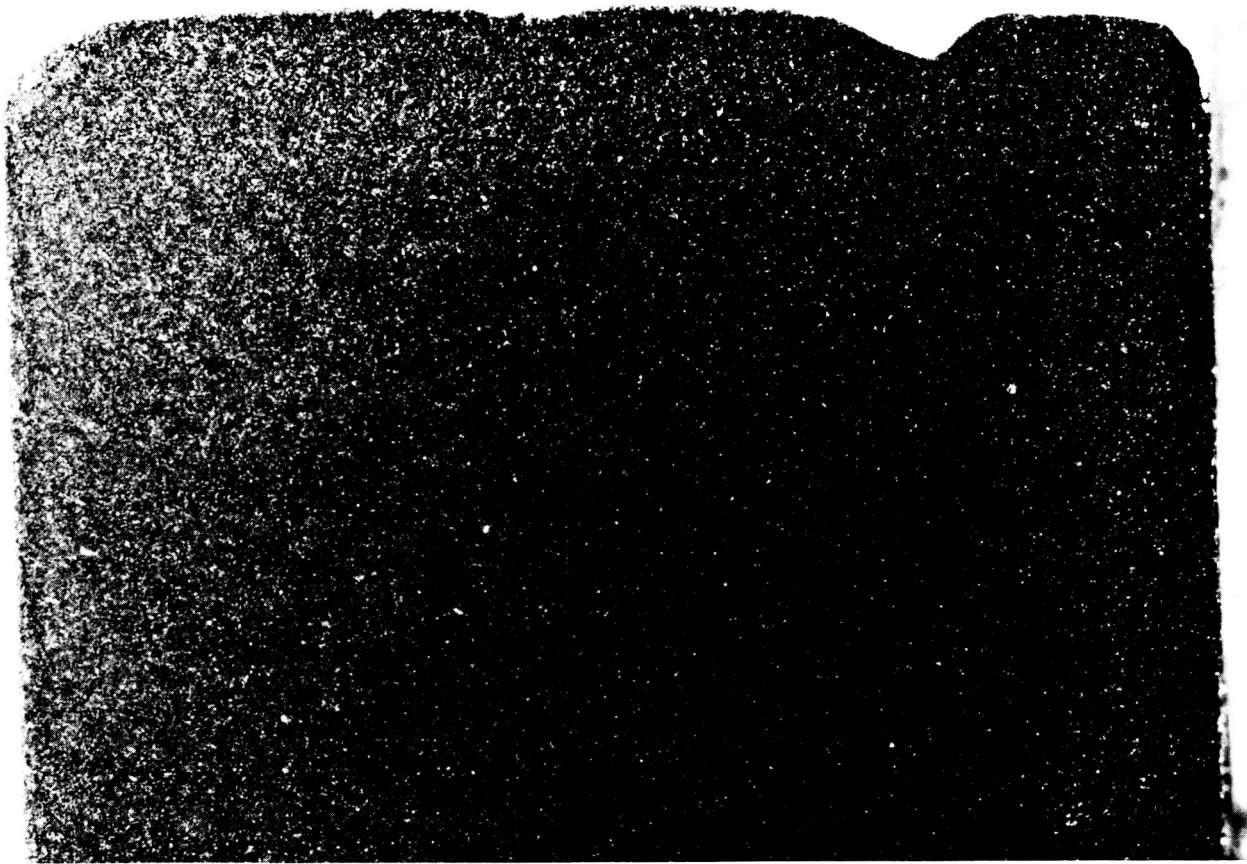
Fig. 26. Tantalum carbide wedge face after exposure to high-velocity lithium for 100 hr at 2000°F
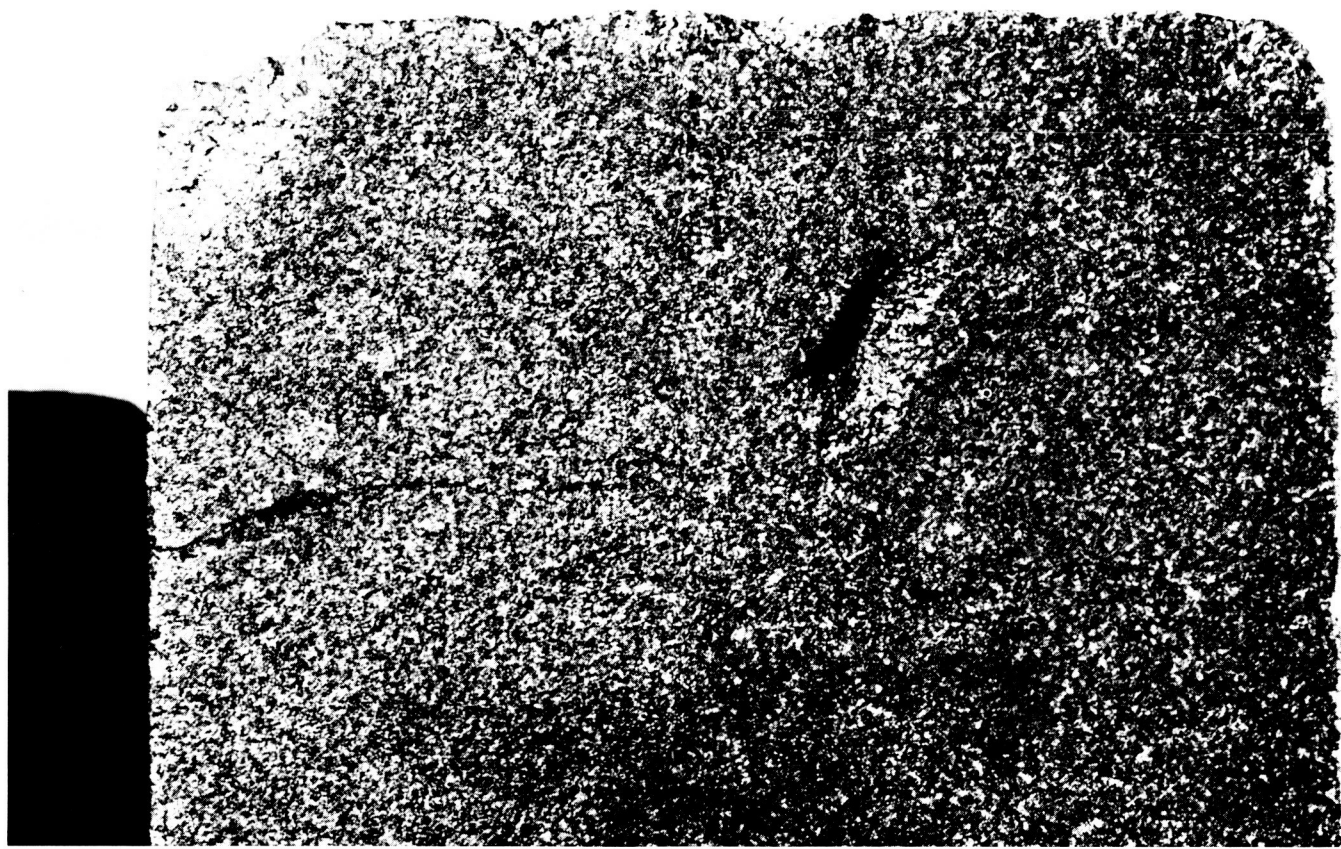
Fig. 27. Titanium carbide wedge face after exposure to high-velocity lithium for 100 hr at 2000°F

The tantalum carbide appeared to have reacted chemically with the lithium to give an overall dissolution of the material. Examination of Figs. 21 and 26 reveals a smoothed and rounded tip as opposed to the more jagged features of the tungsten or zirconium carbide. The high percentage of tantalum in one of the post-test lithium analyses and tantalum deposits on the tungsten and zirconium carbide specimens indicate an extensive reaction. Whereas the discoloration of the tungsten and the zirconium carbide was a change from a silvery to gold color the surface of the tantalum carbide lost its normal gold color and became blackened.

Perhaps the least damaged carbide was the titanium carbide which had very little material loss from the tip. However, as can be seen in Figs. 22 and 27 extensive cracking and flaking occurred. The microstructure before and after exposure is shown in Fig. 28 and can be compared to the microstructure resulting from long term static exposure, Fig. 29. The attack was intergranular. The rounded corners along the cracks suggest that dissolution of impurities which segregated at the grain boundaries may have occurred.

The results for the carbides are especially significant since 2000 hour exposure to static lithium at 2000°F produced less mechanical damage than the 100 hour exposure, to impinging lithium in this test. This result was for the same batch of hot-pressed material so purity differences were not an important factor. On the basis of these tests the use of the softer Cb-1%Zr for the separator appears more promising than use of these hard carbides or of thoriated tungsten.

B. Flow Nozzles

A cross section of the flow nozzles after the test is shown in Fig. 30. The velocity in the nozzles during the 2000°F portion of the test ranged from 180 to 270 ft/s. The diameter of the nozzles was measured and found to be equal to the pretest value (0.1095 in.). The original tool marks can also be seen in Fig. 31, which provides a closeup of each nozzle. Some pitting or grain removal is evident on both nozzles. However, it is not clear whether these defects existed prior to testing or resulted from it. Other machined surfaces of the Cb-1%Zr which were not exposed to lithium show similar defects.

(a) BEFORE EXPOSURE (×400 MAGNIFICATION)

(b) AFTER EXPOSURE (×100 MAGNIFICATION)

CRACK

EDGE OF TEST
SPECIMEN

(c) AFTER EXPOSURE (×400 MAGNIFICATION)

CRACK
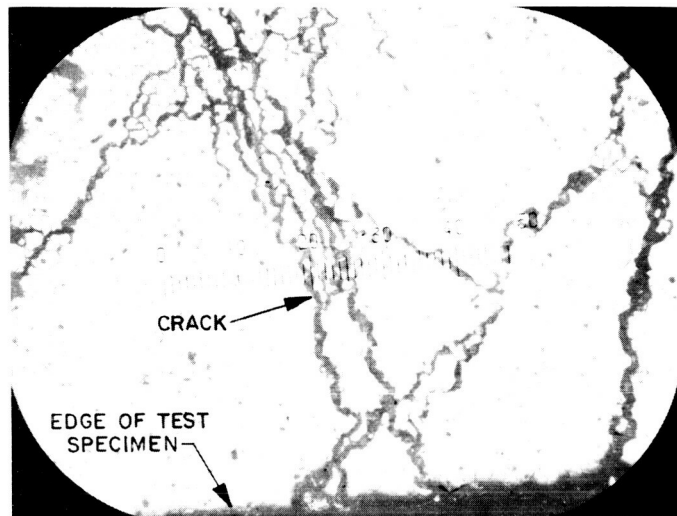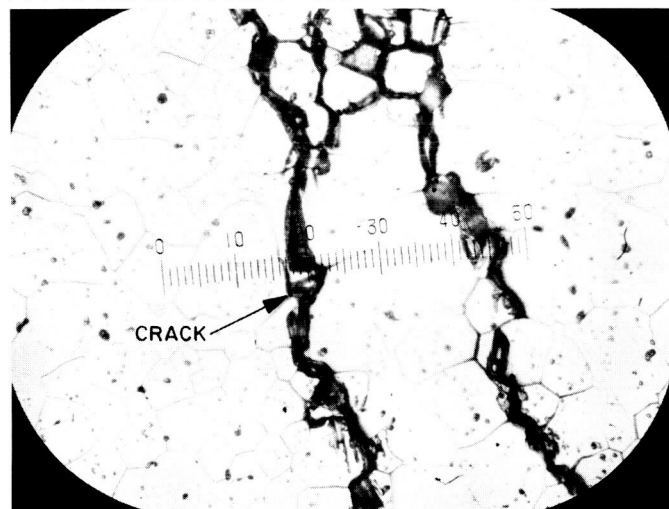
Fig. 28. Titanium carbide (TiC) before and after exposure to 2000°F high-velocity lithium for 100 hr
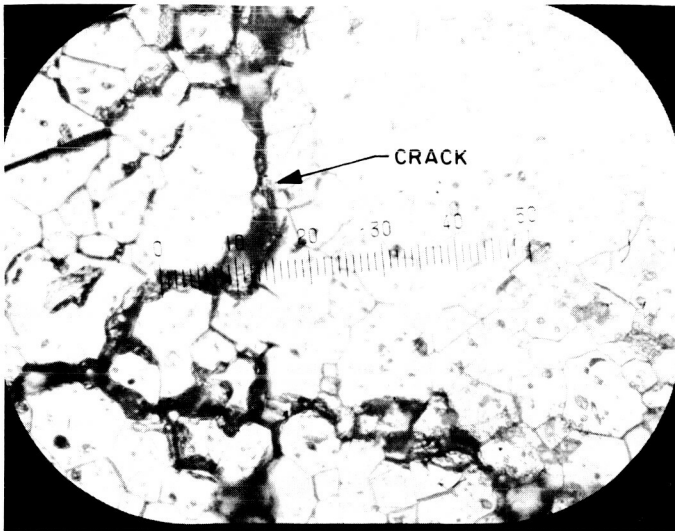
Fig. 29. Titanium carbide (TiC) after exposure to 2000°F
static lithium for 2000 hr ($\times$ 400 magnification)
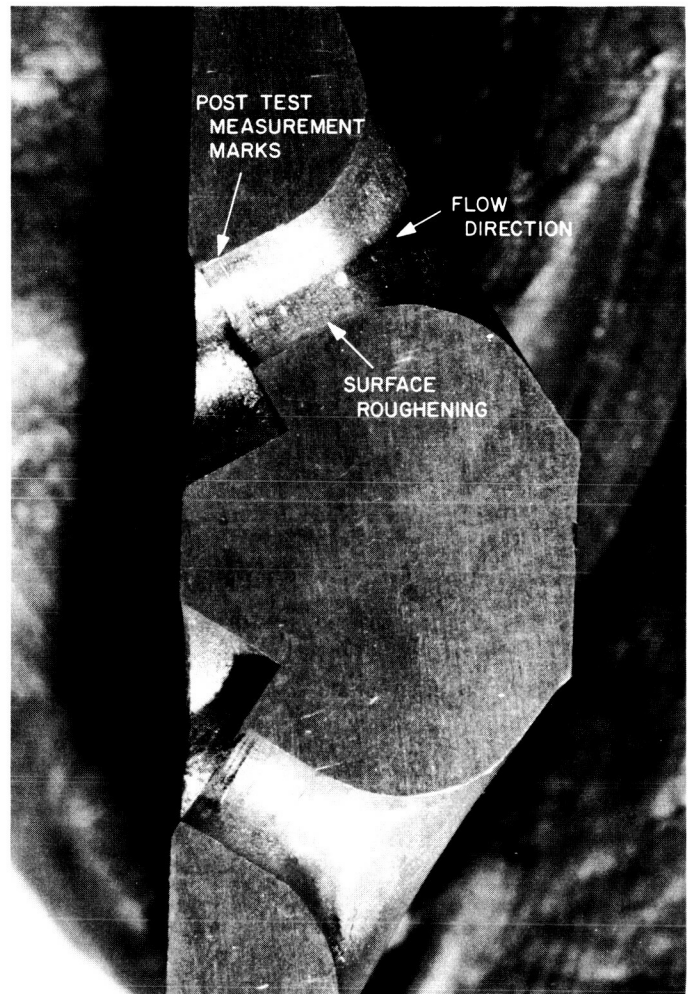
Fig. 30. Cross-section of Cb-1%Zr flow nozzles after
100 hours operation with 2000°F lithium. Velocity
range of 180–270 ft/s

DEPOSIT AND/OR
GRAIN REMOVAL
AT LOCATION OF
ZrC PLUG →
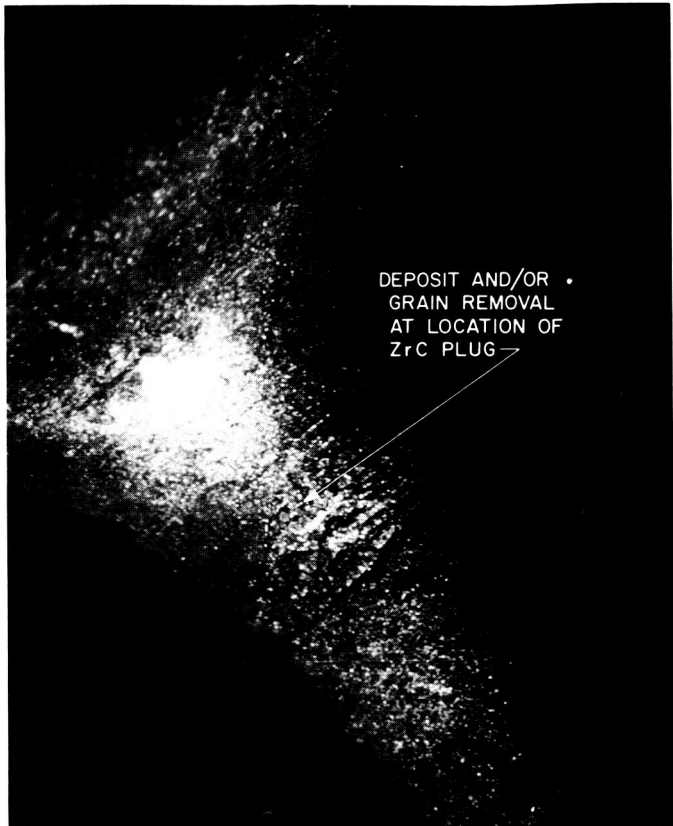
Fig. 31. Cross-section of flow nozzles after testing (0.1095-in. diameter)

V. Conclusions

The results of high velocity flow and impingement of 2000°F lithium support the use of Cb-1%Zr alloy for containment and as a possible separator material for the liquid MHD power system. Further testing of this alloy at higher velocities is required for a quantitative estimate of material loss for long periods of operation. TaC, TiC, ZrC and W-2%ThO$_2$ do not appear to be suitable as separator materials in a lithium system.

All high temperature components to be used in further erosion tests at higher velocities performed in a satisfactory and predictable manner and are suitable for their intended service.

References

1. Elliott, D., Cerini, D., and Weinberg, E., "Liquid Metal MHD Power Conversion," *Space Power Systems Engineering, Progress in Astronautics and Aeronautics, Vol. 16*, Academic Press, New York, Feb. 1966.

2. Elliott, D., Cerini, D., Hays, L., O'Connor, D., Weinberg, E., "Liquid MHD Power Conversion," Space Programs Summary 37-28, Vol. IV, Jet Propulsion Laboratory, Pasadena, Calif., June 1, 1964.

3. Gill, W., Vanek, R., et al., "Mass Transfer in Liquid Lithium Systems" *AIChE Journal*, Vol. 6, No. 1, March 1960.

4. Elliott, D., Cerini, D., and Hays, L., "Liquid MHD Power Conversion," Space Programs Summary 37-41, Vol. IV, Jet Propulsion Laboratory, Pasadena, Calif., June 1966.

5. Thurber, W., *Metals and Ceramics Division Annual Report for Period Ending June 30, 1964*, Section 14, ORNL-3670, TID 4500, 34th Ed. p. 83. Oak Ridge National Laboratory, Oak Ridge, Tennessee, Sept. 1966.

6. Cook, W., *Corrosion Resistance of Various Ceramics and Cermets to Liquid Metals*, ORNL-2391, Oak Ridge National Laboratory, Oak Ridge, Tennessee.

7. Dunn, W., Bonilla, C., et al., "Mass Transfer in Liquid Metals," *AIChE Journal*, Vol. 2, No. 2, June 1956.

8. Traylor, E., Burris, L., and Geankopolis, C., "Mass Transport from a Uranium Sphere to Liquid Cadmium in Highly Turbulent Flow," *I & EC Fundamentals*, Vol. 4, No. 2, May 1965.

9. Davis, J. P., and Kikin, G. M., "Lithium Boiling Potassium Rankine Cycle Test Loop Operating Experience," To be presented at Second Intersociety Energy Conversion Engineering Conference, Aug. 13–17, 1967.

10. Overman, A. Y., et al., *LCRE Non-Nuclear Systems Test Final Report*, Report No. PWAC-402, Part IV, Pratt and Whitney Aircraft, Middleton, Connecticut, Oct. 1965.

11. Abramovich, G., *The Theory of Turbulent Jets*, MIT Press, Cambridge, Mass., 1963.